JOURNAL OF GEOPHYSICAL RESEARCH, VOL. 97, NO. C4, PAGES 5423–5445, APRIL 15, 1992

Variation of the Western Equatorial Pacific Ocean, 1986–1988

THIERRY DELCROIX, GÉRARD ELDIN, AND MARIE-HÉLÈNE RADENAC

Institut Français de Recherche Scientifique Pour le Développement en Coopération (ORSTOM) Nouméa, New Caledonia

JOHN TOOLE

Woods Hole Oceanographic Institution, Woods Hole, Massachusetts

ERIC FIRING

University of Hawaii, Honolulu

Twenty-one oceanographic sections made along 165°E during 1984–1988 provide a unique picture of the 1986–1987 El Niño and the subsequent La Niña in the western equatorial Pacific. The mean of six cruises from January 1984 through June 1986, a relatively normal period, provides a reference with which the later sections are compared. The net warm water transport across 165°E within 10° of the equator was small in this mean reference section: 7×10^6 m^3 s^{-1} to the east. In December 1986, strong westerly winds at and to the west of 165°E increased the net eastward transport of warm water to 88×10^6 m^3 s^{-1}, and the 1986–1987 El Niño was underway. During the following 2 years the net transport varied widely and rapidly; the extrema were 56×10^6 m^3 s^{-1} to the east and 58×10^6 m^3 s^{-1} to the west. Changes in the stratification along 165°E were correspondingly large, reflecting both the geostrophic balance of the strong zonal currents and the changes in the volume of warm water in the western equatorial Pacific. The anomaly of warm water volume corresponded closely to the time integral of the warm water transport across 165°E. Local wind forcing and remotely forced waves were both important causes of the transport fluctuations. Winds, precipitation, and currents were all important factors determining the depth of the surface mixed layer and the thickness of the underlying barrier layer. The way in which these factors interact is a strong function of latitude.

1. INTRODUCTION

The El Niño–Southern Oscillation (ENSO) phenomenon involves the coupled evolution of the tropical Pacific Ocean and the global atmosphere. The large-scale zonal gradient of sea surface temperature (SST) in the equatorial Pacific, with temperatures in the west 7°C or more higher than in the east [e.g., *Levitus*, 1982, Figure 12], is caused by the westward wind stress on the ocean: the trade winds. The low-latitude wind field is, in turn, intimately related to the spatial pattern of SST. El Niño, as *Bjerknes* [1966] first noted, represents an instability of this ocean-atmosphere system in which the trade winds and zonal SST gradient undergo a mutual collapse.

Initial observational work on El Niño was directed toward the eastern Pacific, where surface temperature anomalies during ENSO are maximum [e.g., *Rasmusson and Carpenter*, 1982]. Notable in these efforts was the study of *Leetmaa et al.* [1987] who, using cruise data, described the time evolution of the ocean stratification and circulation along 95°W during the 1982–1983 El Niño. More recently, it was recognized that pronounced atmospheric heating by deep convection is closely associated with regions where SST is warm [e.g., *Gill and Rasmusson*, 1983]. This recognition has focussed attention on the western Pacific, where SST frequently exceeds 29°C. One key, underlying the ongoing International Tropical Ocean–Global Atmosphere (TOGA) [*World Climate Research Program (WCRP)*, 1985] program, is the question: what processes control the spatial distribution of SST in the equatorial Pacific Ocean (and, in turn, the pattern of atmospheric forcing). Of particular concern are the processes affecting the extent of the warmest surface waters.

The present paper will address this question by documenting the time-varying zonal circulation and associated stratification in the western equatorial Pacific during the 1986–1987 El Niño and the subsequent cold period in 1988, variously called the cold phase of ENSO, La Niña (which will be used here), or anti–El Niño. Specifically, we describe results from a series of 21 oceanographic cruises in the equatorial Pacific along longitude 165°E, spanning the period January 1984 to October 1988 (Figure 1, Table 1).

The section which immediately follows provides an overview of the 165°E field programs, data sets, and analysis methods. As background to the study of the 1986–1988 ENSO, we first review the mean distributions along 165°E during January 1984 through June 1986 (section 3). To further set the stage, we briefly discuss the large scale evolution of the tropical Pacific Ocean and atmosphere during the 1986–1988 ENSO in section 4. A detailed chronological description together with tentative interpretation of the variability at 165°E will follow (section 5). Air-sea interactions are of course sensitive to the characteristics of the ocean surface mixed layer. The time evolution of the upper ocean stratification at 165°E during this period is discussed in section 6, with particular attention paid to the relative contributions of temperature and salinity. We conclude with a general discussion of the western Pacific warm water pool as it changed during the 1986–1988 ENSO (section 7).

Paper number 92JC00127.
0148-0227/92/92JC-00127$05.00

2. DATA AND METHODS

The primary data sets we will use are shipboard measurements, principally along 165°E, from six independent research programs (Table 1). Repeated oceanographic cruises along 165°E were begun in January 1984 by the Institut Français de Recherche Scientifique pour le Développement en Coopération (ORSTOM) Groupe SURTROPAC (Surveillance Trans-Océanique du Pacifique), based in Nouméa, New Caledonia. Ten semiannual SURTROPAC cruises, nominally during January and July of each year, are discussed here. The ORSTOM observational effort was augmented in 1987 by the PROPPAC (Production Pélagique dans le Pacifique) program which ran cruises in the spring and fall. Here we present results from three PROPPAC expeditions (September 1987 and 1988, May 1988). The other major program involving repeated oceanographic measurements along 165°E was the U.S.–People's Republic of China (US-PRC) Joint Program on Air-Sea Interaction Studies in the Tropical Western Pacific. Staged from Guangzhou, China, this program included five sections on 165°E dur-

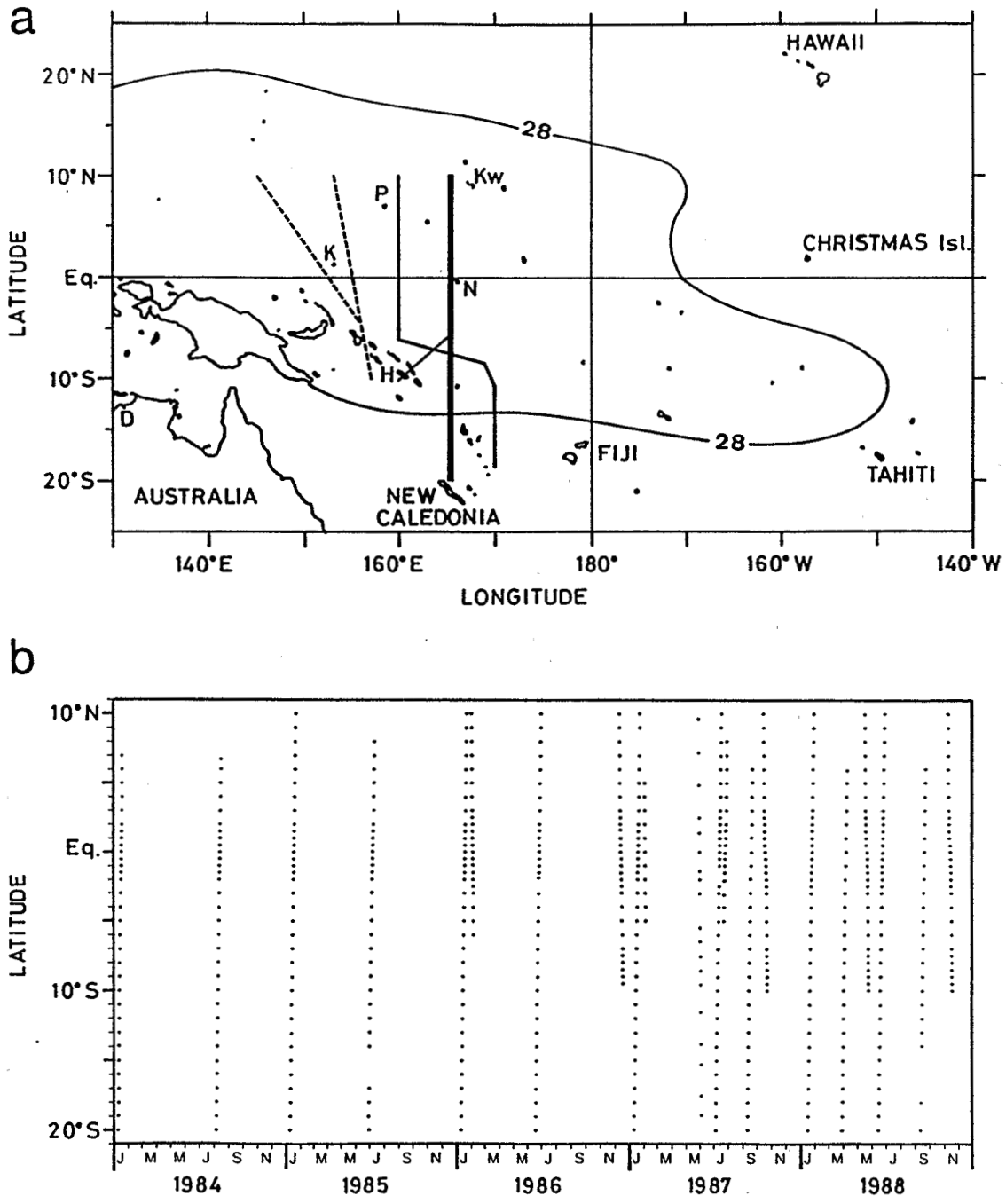

Fig. 1. (*a*) Location of temperature, salinity and velocity sections near 165°E (solid lines), and of XBT tracks within 145°–160°E (dashed lines). Overplotted is the climatological mean position of the 28°C isotherm bounding the western Pacific warm pool, as derived from *Levitus* [1982]. From north to south, one- or two-letter abbreviations mark the positions of Kwajalein (Kw), Pohnpei (P), Kapingamarangi (K), Nauru (N), Honiara (H), and Darwin (D). (*b*) Time–latitude map of cruise stations near 165°E.

TABLE 1. Cruises Near 165°E During 1984–1988

	Cruise	Origin*	Time	Section Track
1	SURTROPAC 1	ORSTOM	Jan. 10–20, 1984	20°S–7°N at 165°E
2	SURTROPAC 2	ORSTOM	Aug. 5–15, 1984	20°S–6°40'N at 165°E
3	SURTROPAC 3	ORSTOM	Jan. 9–21, 1985	20°S–10°N at 165°E
4	SURTROPAC 4	ORSTOM	June 28 to July 9, 1985	20°S–8°N at 165°E
5	SURTROPAC 5	ORSTOM	Jan. 10–26,1986	20°S–10°N at 165°E
6	US-PRC 1	WHOI-SOA	Jan. 30 to Feb. 5, 1986	10°N–6°S at 165°E
7	SURTROPAC 6	ORSTOM	June 17–27, 1986	20°S–10°N at 165°E
8	US-PRC 2	WHOI-SOA	Dec. 8–16, 1986	10°N–6°S at 165°E, then to 10°S at 160°E
9	SURTROPAC 7	ORSTOM	Jan. 10–27, 1987	20°S–10°N at 165°E
10	JENEX 1	JAMSTEC	Feb. 1–4, 1987	5°N–5°S at 160°E
11	SAGA 2	SIO-IAG	May 23 to June 6, 1987	20°N–5°S at 160°E, then 10°S–19°S at 170°E
12	SURTROPAC 8	ORSTOM	July 2–15, 1987	20°S–10°N at 165°E
13	TEW3	PMEL	July 20–26, 1987	5°S–6°N at 165°E
14	PROPPAC 1	ORSTOM	Sept. 9–20, 1987	20°S–6°N at 165°E
15	US-PRC 3	WHOI-SOA	Oct. 13–22, 1987	same as for US-PRC 2
16	SURTROPAC 9	ORSTOM	Jan. 16–28, 1988	20°S–10°N at 165°E
17	PROPPAC 2	ORSTOM	March 28 to April 8, 1988	20°S–6°N at 165°E
18	US-PRC 4	WHOI-SOA	May 15–23, 1988	10°N–6°S at 165°E, then to 10°S at 163°E
19	SURTROPAC 10	ORSTOM	June 14–27, 1988	20°S–10°N at 165°E
20	PROPPAC 3	ORSTOM	Sept. 11–22, 1988	20°S–6°N at 165°E
21	US-PRC 5	WHOI-SOA	Nov. 8–17, 1988	same as for US-PRC 4

*Abbreviations are ORSTOM, Institut Français de Recherche Scientifique Pour le Développement en Coopération; WHOI, Woods Hole Oceanographic Institution; SOA, State Oceanic Administration; JAMSTEC, Japan Marine Science and Technology Center; SIO, Scripps Institution of Oceanography; IAG, Institute of Applied Geophysics; PMEL, NOAA Pacific Marine Environmental Laboratory.

ing the period of interest here (Table 1). Supplementing these series of cruises are three individual occupations of meridional sections by other programs: the SAGA 2 cruise [*Talley and Collins*, 1988] which ran chiefly along 160°E; the Transports of Equatorial Waters (TEW) cruise leg 3 of the *Oceanographer* [*Mangum et al.*, 1991]; and the JENEX 1 cruise (K. Muneyama, personal communication, 1990).

Each expedition obtained vertical profiles of temperature, salinity, and horizontal velocity at selected sites ranging between 20°S and 10°N (Figure 1), except that no velocity measurements were made on the SAGA 2, JENEX 1, and US-PRC 1 cruises. Temporal sampling density, while exceptional for shipboard programs, still left much variability unresolved. Therefore we will also use complementary observations with better time resolution but poorer spatial resolution.

2.1. *Temperature and Salinity*

Standard hydrographic observations were obtained with wire-lowered conductivity-temperature-depth (CTD) instruments. The reader is referred to the data reports by *Blanchot et al.* [1987], *Eldin* [1989], *Cook et al.* [1990], *Talley and Collins* [1988], and *Mangum et al.* [1991] for specifics. Our focus here is on the upper 1000 m of the water column, an interval sampled by all but one cruise. (The JENEX 1 data extend to 500 m.) Potential temperature–salinity plots of the combined data set indicate that upper ocean salinity uncertainty is generally less than 0.01 psu. Given the sizable meridional salinity gradients on isotherms along 165°E, it is difficult to be more quantitative; cruise to cruise differences might equally reflect meridional displacements of water masses as calibration error. For our present analysis, this uncertainty is inconsequential.

2.2. *Velocity*

Horizontal velocity measurents between the surface and 600 m were obtained on the SURTROPAC and PROPPAC cruises with a profiling current meter system as described by *Delcroix et al.* [1987]. A comparison of profiler velocity data with discrete measurements from a current meter mooring deployed at 0°, 165°E, with both computed relative to 300 dbar, gave a global mean ± standard deviation difference of 1±12 cm s^{-1} for the 45 comparisons analyzed. The rms differences decreased from 14 to 4 cm s^{-1} between 10 and 200 dbar. A subsequent comparison between profiler measurements and shipboard acoustic Doppler current profiler (ADCP) measurements at 15 stations along 165°E, 10°S to 7°N, gave mean ± standard deviation differences of 2±8 cm s^{-1} and 0±6 cm s^{-1} for the zonal and meridional velocity components, respectively, when both measurements were referenced to the layer 16–240 m (T. Delcroix et al., Comparison of profiling current meter and shipboard ADCP measurements in the western equatorial Pacific, submitted to *Journal of Atmospheric and Oceanic Technology*, 1992, hereinafter Delcroix et al., 1992). The differences increased to 6±11 cm s^{-1} and 0±9 cm s^{-1} when the ADCP data were referenced to the Earth using Global Positioning System (GPS) navigation and the profiler measurements were referenced to 600 dbar.

The error involved in treating the SURTROPAC velocities relative to 600 dbar as if they were absolute can also be estimated with current profiles obtained during the PEQUOD experiment along 159°W [*Firing*, 1987]. There, the 16-month mean zonal currents at 600 m were in the range ±10 cm s^{-1}, and the standard deviation over the 16 months was also about 10 cm s^{-1}. If we assume similar flow characteristics at 165°E, errors in the present transport estimates caused by mean and fluctuating currents at 600 m, when in phase, sum to about 2×10^6 m^3 s^{-1} per degree latitude, per 100 m depth. We expect these errors to be decorrelated (or in some cases inversely correlated) over a few degrees latitude, the scales of the currents and equatorial waves causing the 600 m currents. The error in transport through the section in a given depth range cannot be estimated with any

great confidence. The contribution from the reference level assumption is simply the product of the thickness of the layer, the latitude range, and the average over that latitude range of the zonal current at 600 m. We do not know the statistics of this average current, however. Supposing the 10°N to 10°S average current at 600 m to be 2 cm s^{-1}, for example, gives a transport error of 4×10^6 m^3 s^{-1} per 100 m depth. Taking the meridional mean difference in zonal velocity component from Delcroix et al. (1992), 6 cm s^{-1}, gives an estimated transport error of 12×10^6 m^3 s^{-1} per 100 m depth.

Acoustic Doppler current profilers were used on the US-PRC and TEW 3 cruises. Both the Chinese ships and the *Oceanographer* were equipped with RD Instruments 150-kHz profilers. Absolute velocities were estimated by combining satellite navigation with the ADCP measurements as described by *Bahr et al.* [1989]. The ADCP depth range was variable but typically extended from 20 to 300 m.

The main uncertainty in the ADCP absolute velocity estimates used here is due to difficulties in calibrating the orientation of the transducer relative to the gyrocompass. We believe it is unlikely that this error exceeds 1° when averaged over a day or more [*Bahr et al.*, 1989, 1990]. Given the 4 m s^{-1} average speed of the US-PRC ships along the 165°E section, including stops for CTD stations, this maximum orientation error would cause an error of 7 cm s^{-1} in the zonal velocity estimates. If the gyrocompass component of the error were constant along the section, then the velocity error would also be constant and would bias transport estimates in a 100-m-thick layer by 0.8×10^6 m^3 s^{-1} per degree latitude. Note that this error, unlike the error in the mechanical profiler estimates due to the 600 m reference level, could persist as a bias all along the 165°E section.

2.3. Supplementary Data

Since 1979 an expendable bathythermograph (XBT) ship of opportunity program [*Meyers and Donguy*, 1980] has obtained upper ocean temperature data along a track between Japan and New Caledonia; the 1984–1989 data were kindly provided by the International TOGA Subsurface Data Center in Brest, France. The ship routes, which are inclined slightly to the northwest, cross the equator between 140°E and 160°E (Figure 1). Temperature profiles down to 400 m are available along the track at roughly 3–4 drops per month in each 2° latitude bin during the time interval examined here. Corresponding 0/400 dbar dynamic heights were computed using the mean *Levitus* [1982] temperature-salinity (T-S) relation. For the 1984–1986 period the rms error was 2 dyn cm [*Delcroix et al.*, 1987]; changes in the T-S relation during the 1986–1988 period increased the error considerably [*Hénin*, 1989].

Daily mean sea level data are available from the network of tide gauges maintained at islands in the tropical Pacific by K. Wyrtki and colleagues at the TOGA Sea Level Center in Honolulu, Hawaii. Here we examine the records from the islands of Kwajalein, Nauru, Kapingamarangi and Christmas, and from Honiara in the Solomon Islands (Figure 1). The time series of relative sea level from these sites were referenced to 0/1000 dbar dynamic height data using the method of *Wyrtki* [1974]. Agreement between our dynamic height data along 165°E and the leveled tide gauge data from Kwajalein, Nauru and Honiara is excellent (Figure 2); the differences between dynamic heights and leveled gauge data had standard deviations of 7.5–11 cm. The sea level records from Pohnpei and Kapingamarangi were strongly correlated with the series from Kwajalein and Nauru, respectively. Consequently, they will not be shown here.

2.4. Warm Water Volume and Zonal Transport

To test the hypothesis that most of the change in warm water volume west of 165°E within 10° of the equator is caused by changes in the zonal transport across 165°E, we estimated both the volume and the time integral of the transport. The volume was calculated using the ship of opportunity XBT data west of 165°E. The mean depth of the 25° isotherm at each latitude was multiplied by the distance from the 165°E meridian to the western boundary (defined by the north coast of New Guinea and the 130°E meridian), and the product was integrated from 10°S to 10°N. The transport across 165°E of water with $\sigma_t > 23.5$ (an isopycnal close to the 25° isotherm) was estimated primarily from the direct current measurements on cruises (Figure 3). Because there were no direct measurements on the JENEX 1 and SAGA 2 cruises, geostrophic current estimates were used for these cruises poleward of 3°, the 165°E equatorial mooring record was used to approximate the currents between 0.5°S and 0.5°N, and currents in the ranges 0.5°–3°N and 0.5°–3°S were interpolated linearly between the poleward geostrophic estimate and the equatorward moored measurement. The estimates of 10°S to 10°N transport for each cruise were then linearly interpolated in time, starting with SURTROPAC 5, with the following exception. In the second half of 1986, the transport was approximated as the SURTROPAC 6 value for the 2 months following that cruise, then as zero for the following 2 months, and then as the US-PRC 2 value until the US-PRC 2 cruise. These transport changes are consistent with changes in sea level slope, Nauru to Honiara and Nauru to Kwajalein (Figure 2).

3. MEAN STRUCTURE AT 165°E

The water mass characteristics and circulation of the tropical Pacific Ocean around longitude 165°E have previously been discussed by *Barnes et al.* [1948], *Rotschi et al.* [1972], *Magnier et al.* [1973], *Delcroix et al.* [1987], and *Toole et al.* [1988], among others. For the present study, we constructed an average section of temperature, salinity, and zonal velocity from the first six SURTROPAC transects made between January 1984 and June 1986 [see *Delcroix et al.*, 1987]. This average is superior to earlier climatologies in having high meridional resolution (50–100 km) and direct observations of velocity as well as temperature and salinity. In subsequent paragraphs, this mean section will be used as a reference for each of the synoptic occupations of 165°E.

It is difficult to establish how representative of the long-term mean is this average of just six semiannual cruises. Previous studies of the seasonal variability of the western equatorial Pacific [*Wyrtki*, 1974; *Tournier*, 1989; *Picaut and Tournier*, 1991] indicate that observations in January and July are at opposite phases of the seasonal cycle; hence our average section should not have significant seasonal bias. On longer time scales, the Southern Oscillation Index (SOI) for the period mid-1983 to mid-1986 (Figure 4) suggests that little interannual variability occurred in the large scale wind field during the time of the first six SURTROPAC cruises; the SOI fluctuated around zero with no significant trend. It

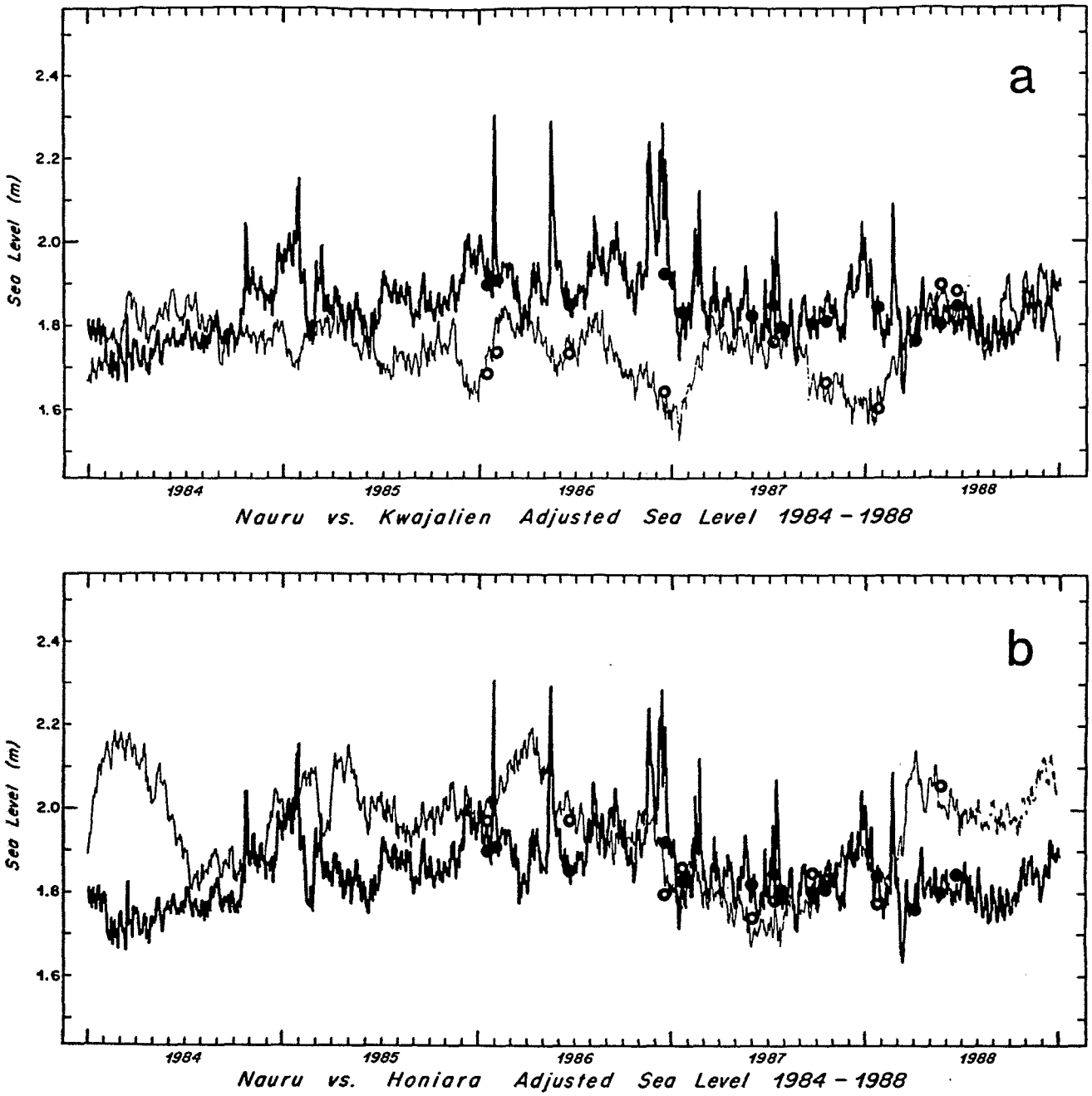

Fig. 2. Time series plots of sea level and 0/1000 dbar dynamic height from Kwajalein, Nauru, and Honiara for (*a*) Kwajalein and Nauru and (*b*) Honiara and Nauru. In both cases, Nauru is denoted with the bold line. The solid (Nauru) and open (Kwajalein and Honiara, respectively) circles mark the 165°E cruise data-derived dynamic heights at the latitudes of the island stations. The sea level records were referenced with the dynamic height data [*Wyrtki*, 1974]. Note that periods of westerly winds at Nauru are frequently associated with spikes in sea level caused by setup in the harbor where the gauge is located [*Wyrtki*, 1984].

follows that the averaged section is probably not strongly biased toward El Niño or La Niña conditions. This claim is supported by comparison of the six-cruise mean 0/1000 dbar dynamic height data with the mean section of *Toole et al.* [1988] constructed from historical hydrographic data (Figure 5). The two height fields agree well; the rms difference is only 0.6 dyn cm over the latitude range 10°N to 8°S.

Surprisingly, the dynamic height data of *Levitus* [1982] for this region are approximately 2 dyn cm lower than the other two height fields (Figure 5). In addition, there is no indication in the Levitus data of the marked trough around 11°S which separates the South Equatorial Current (SEC) and South Equatorial Countercurrent (SECC) [*Oudot and Wauthy*, 1976]. We have no definite explanation for the discrepancy in overall level, but it may be connected with a difference in zonal averaging; the Toole et al. section is averaged over 153°–170°E, whereas the Levitus section is

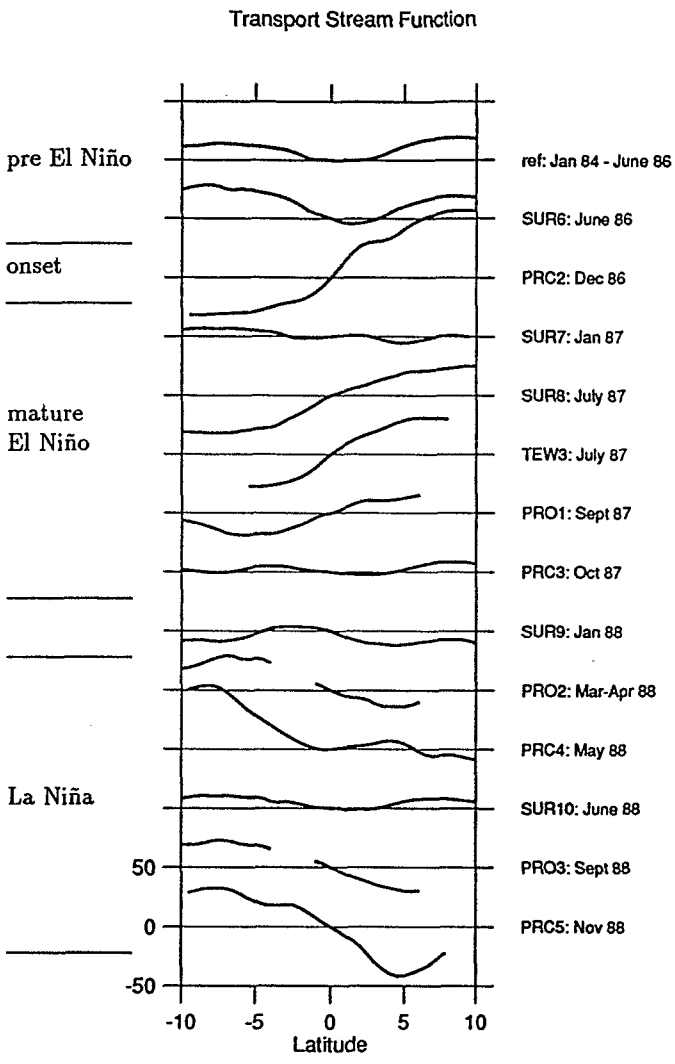

Fig. 3. Transport stream function for waters above 23.5 σ_t for each of the cruises on 165°E with direct current measurements. The PRC and TEW measurements are absolute; the others are relative to 600 dbar. Transport stream function increases to the north for eastward currents. Successive curves are offset by 50×10^6 m^3 s^{-1} at the equator.

averaged over 160°–170°E. We suspect that low data density and the long objective mapping scale contributed to the differences around 11°S.

The surface layer in the western Pacific near the equator is, on average, uniformly warm, in contrast to the mean conditions in the central [*Wyrtki and Kilonsky*, 1984] and eastern equatorial Pacific [*Hayes et al.*, 1986]. No indication of equatorial upwelling is seen in the mean distribution of SST at 165°E (Figure 6). Average ocean temperatures greater than 29°C extend meridionally from 6°N to 10°S, and in depth to 60 m. *Levitus* [1982] found $SST > 29$°C from about 5°N to 10°S at 165°E; *Tournier* [1989] obtained similar results from XBT data gathered along the Nouméa-Japan shipping track. The *Toole et al.* [1988] averaged section for the band 153°–170°E has a somewhat smaller extent of warm water: 1°–7°S. Information about the seasonal meridional migration of this warm water is given by *Tournier* [1989] and *Delcroix and Masia* [1989].

The averaged temperature section shows an almost isothermal upper layer (temperature within 1°C of SST) reaching as much as 80 m depth within 10°N to 10°S (Figure 6). Below 100 m is a well-defined thermocline centered about the 20°C isotherm with ridges and troughs reflecting the zonal geostrophic upper ocean currents. The weakening of the thermocline within a degree of the equator is associated with the equatorial undercurrent (EUC) [*Hayes*, 1982]. At somewhat greater depths ($T < 15$°C), the isotherms shoal steeply poleward of 2° latitude as required for geostrophic balance within the North and South Subsurface Countercurrents (NSCC, SSCC).

The mean salinity section (Figure 7) shows low surface salinities north of 2°N and between 6°S and 15°S. These minima are associated with heavy rainfall in the Intertropical Convergence Zone (ITCZ) and the South Pacific Convergence Zone (SPCZ) [*Donguy and Hénin*, 1978; *Merle et al.*, 1969]. In the mean, the surface waters appear homogeneous in salinity down to about 50–60 m depth, slightly shallower than the base of the nearly isothermal surface layer. This difference in thickness between the isothermal and isohaline layers in the western Pacific has been discussed by *Lukas and Lindstrom* [1991] and *Godfrey and Lindstrom* [1989].

Within the thermocline (100–200 m), subtropical high-salinity cores extend equatorward from both hemispheres. The southern core reaches northward past the equator and ends in a region of strong meridional salinity gradient between 1°S and 2°N. The northern core is just identifiable poleward of 8°N. Between these cores is the relatively low salinity water mass that originates near the coast of California and Baja California [*Tsuchiya*, 1968].

The mean section of directly measured zonal currents (relative to 600 m depth; Figure 8) contains all the major flows which characterize the Pacific near-equatorial circulation. The southern edge of the westward North Equatorial Current (NEC) is seen north of 8°N. The mean North Equatorial Countercurrent (NECC) at 165°E lies between 8°N and 1°N with a subsurface velocity extremum (U_{ext}) of 0.4 m s^{-1} at 90 m. Westward surface flow in the South Equatorial Current (SEC) lies in two bands: 1°N to 7°S ($U_{\text{ext}} = -0.4$ m s^{-1}) and from 11°S to 14°S ($U_{\text{ext}} = -0.1$ m s^{-1}). In between is the SECC with maximum eastward velocity of 0.2 m s^{-1}. The main subsurface currents at 165°E are found near the equator. The mean EUC is centered on the equator at 180 m depth with eastward flow extending poleward to ±2° latitude. The NSCC and SSCC's are centered at slightly greater depth (250 m) and higher latitude (±3°), surrounding the westward Equatorial Intermediate Current (EIC) centered on the equator.

The current with the largest transport in the mean section is the SEC, carrying 46.7×10^6 m^3 s^{-1} to the west (Table 2). Less than half of this is compensated by the NECC, with its mean transport of 20.9×10^6 m^3 s^{-1}. It is noteworthy that the total transport of the two subsurface countercurrents exceeds the transport of the EUC and nearly matches that of the NECC.

In their descriptions of currents and hydrography on 165°E, *Delcroix et al.* [1987] and *Delcroix and Hénin* [1988] noted that the 23.5 kg m^{-3} isopycnal (σ_t, or equivalently at these depths, σ_θ) effectively separates surface from subsurface currents. This is roughly the case for the average section as illustrated in Figure 8; the NECC extends below the 23.5 isopycnal, as does the SEC south of 5°S. In the fol-

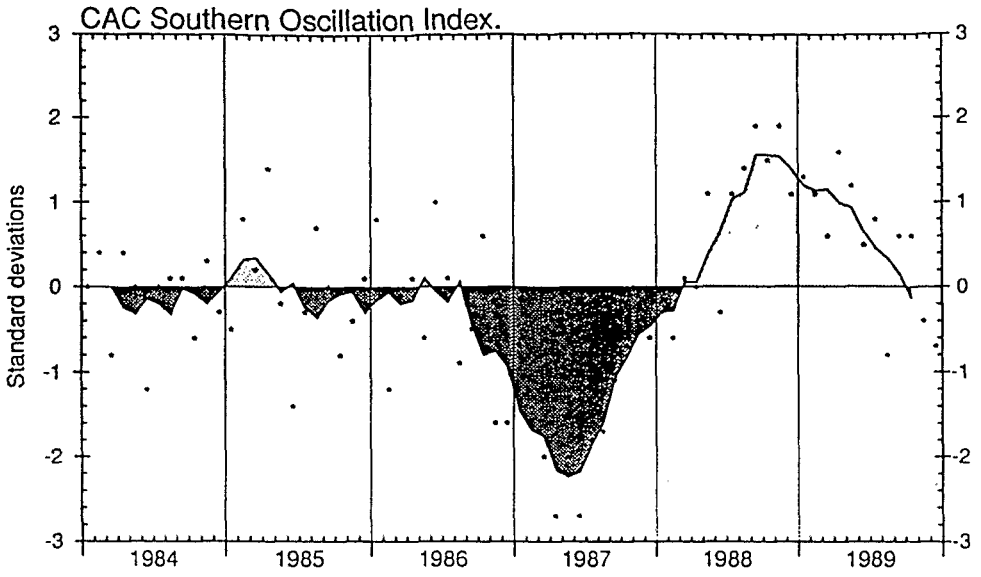

Fig. 4. Five-month running mean of the difference between the standardized sea level pressure anomalies at Tahiti and Darwin (Tahiti minus Darwin). Values are normalized by the mean annual standard deviation. Dots are individual means. (Courtesy of the Climate Analysis Center, Washington, D.C., U.S.A.).

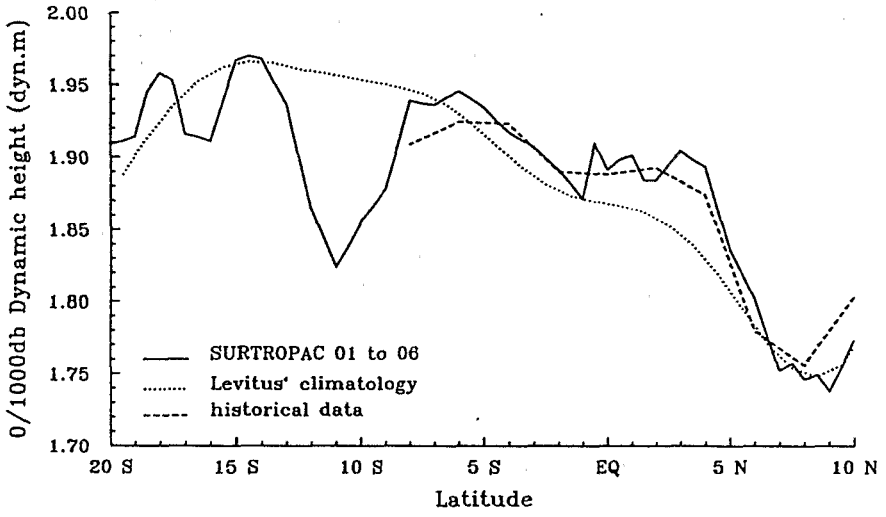

Fig. 5. Reference 0/1000 dbar dynamic height (dynamic meters) section at 165°E, calculated from the 1984–1986 SURTROPAC cruises (solid line). Superimposed are values from the *Levitus* [1982] climatology (dotted line), and the historical data (dashed line) from *Toole et al.* [1988].

lowing, we will also use $\sigma_t = 23.5$ kg m^{-3} to divide surface from subsurface water transports in the synoptic sections. The mean surface layer transport within 10°N to 10°S, using this definition, was 7×10^6 m^3 s^{-1} to the east (Figure 3).

4. Tropical Pacific Variability, 1984–1988

Observations along 165°E characterize only a small fraction of the equatorial Pacific Ocean. To place these data in the context of the basin-wide oceanic and atmospheric variations that occurred during the 1986–1988 ENSO, we review five measures of large-scale variability for this time period: (1) the surface pressure distribution as manifested in the Southern Oscillation Index, (2) the surface wind field, (3) the SST in the near-equatorial zone, (4) the vertical temperature distribution and related upper layer volume of the western equatorial Pacific, and (5) broad meridional scale sea level variations near longitude 165°E.

The SOI stayed near zero from 1984 through mid-1986, and then fell sharply to a minimum around May 1987 (Figure 4). For the succeeding 17 months the SOI gradually rose, crossing zero around March 1988 and peaking in September–October 1988 with the highest value seen since 1973. Thereafter the SOI fell, reaching zero in September 1989. As was mentioned by *Lander* [1989], this sequence resembles the evolution of SOI in *Rasmusson and Carpenter*'s [1982] com-

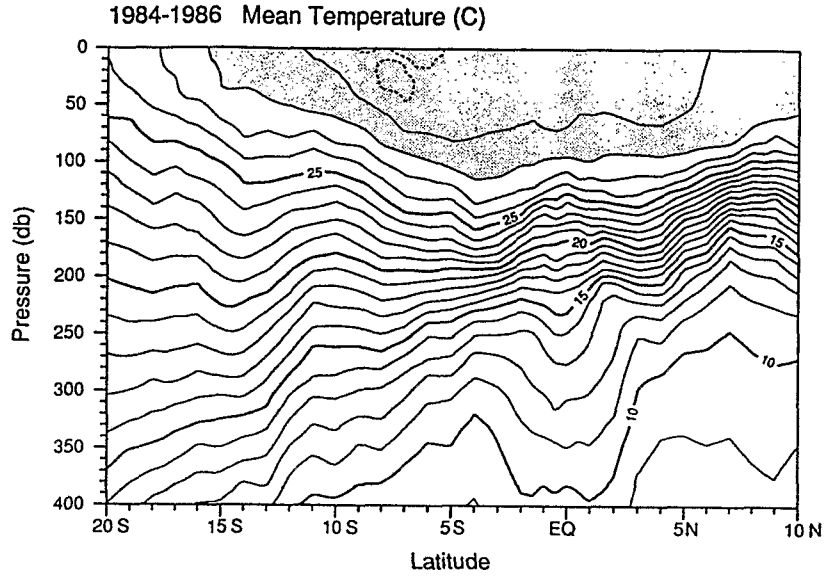

Fig. 6. Reference temperature section at 165°E, calculated from the 1984–1986 SURTROPAC cruises. Contour intervals are 1°C. The broken line denotes the 29.5°C isotherm. Areas with temperature greater than 28°C are shaded.

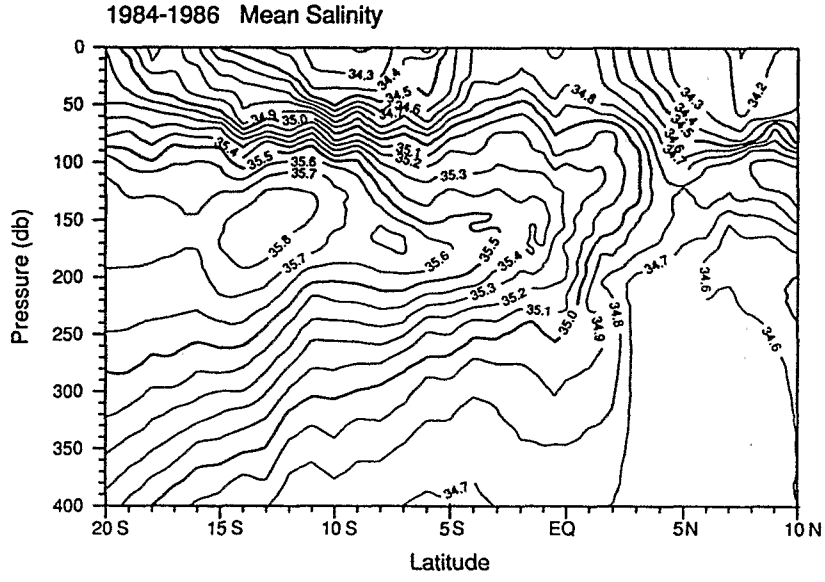

Fig. 7. Reference salinity section at 165°E, calculated from the 1984–1986 SURTROPAC cruises. The contour interval is 0.1 psu.

posite, except that the May 1987 minimum occurred 2–3 months earlier.

Both the local wind variations along 165°E and the large-scale variations across the equatorial Pacific are seen in the zonal pseudo wind stress time series produced at Florida State University (FSU) (Figure 9). At 165°E, seasonal wind cycles are evident in both hemispheres, with maximum trade winds (negative zonal stress) during the respective hemispheric winter seasons. In "normal" years, a weakening or reversal of the trades follows the shift of the ITCZ toward the summer hemisphere. North of the equator, the trades only weaken during boreal summer, but moderate westerlies appear in southern hemisphere summer, extending from near the equator to 12°–13°S. These westerlies are a component of the northwest monsoon which extends eastward from the Indonesian archipelago [*Wyrtki and Meyers*, 1976] (Figure 9*b*).

Starting in July 1986, as the SOI began falling, a strong enhancement of this seasonal cycle was seen; westerly winds appeared at 165°E from the equator to 10°N. These westerlies persisted in time while shifting and expanding southward until March 1987, when they reached 12°S. There were particularly strong northwesterly wind episodes in December 1986 and February 1987. Winds in the next 1-year period were similar in character, but the westerlies were weaker. The area of westerly winds shifted northward in mid-1987 to

TABLE 2. Zonal Current Transports

Cruise	Date	Transport, Sv							
		SECC	SEC	SSCC	EUC	NSCC	NECC	EEC	EIC
1984–1986 Average		7.0	-46.7	6.8	16.1	12.9	20.9		-4.1
SURTROPAC 6	June 1986	9.8	-76.7	5.0	21.3	6.7	25.1		-5.5
US-PRC 2	Dec. 1986	8.1	-3.0	(←	>27.6	→)	57.8	51.6	
SURTROPAC 7	Jan. 1987	6.9	-48.8	6.6	6.7	15.3	13.9	5.1	-14.1
SURTROPAC 8	July 1987	1	-43.9	20.5	17.9	19.4	20.3	30.2	-12.2
TEW 3	July 1987			> 26.0	> 43.0	> 34.7	15.8	44.7	
PROPPAC 1	Sept. 1987	0	-44.6	11.9	17.9	21.7	10.3	22.3	-15.9
US-PRC 3	Oct. 1987	7.6	-25.8	>4.3	0	>18.6	13.2		
SURTROPAC 9	Jan. 1988	12.1	-59.3	10.2	7.6	21.2	19.3		-11.7
PROPPAC 2	March 1988	33.9	-91.3	(←	47.5	→)			-1.0
US-PRC 4	May 1988	5.7	-116.2	(←	42.8	→)	7.8		
SURTROPAC 10	July 1988	13.9	-43.0	8.2	16.7	15.2	17.1		-8.1
PROPPAC 3	Oct. 1988	16.1	-55.8	(←	23.4	→)			
US-PRC 5	Nov. 1988	4.1	-104.0	(←	10.1	→)	39.7		

Cruise names are in italics when the current measurements were absolute and covered approximately the top 300 dbar; the "greater than" sign means that the depth range did not cover the entire current. Measurements on the other cruises were relative to 600 dbar and covered the top 600 dbar. Where a transport estimate is bracketed by parentheses and arrows, it applies to the sum of the SSCC, the EUC, and the NSCC; boundaries between the currents were ill-defined.

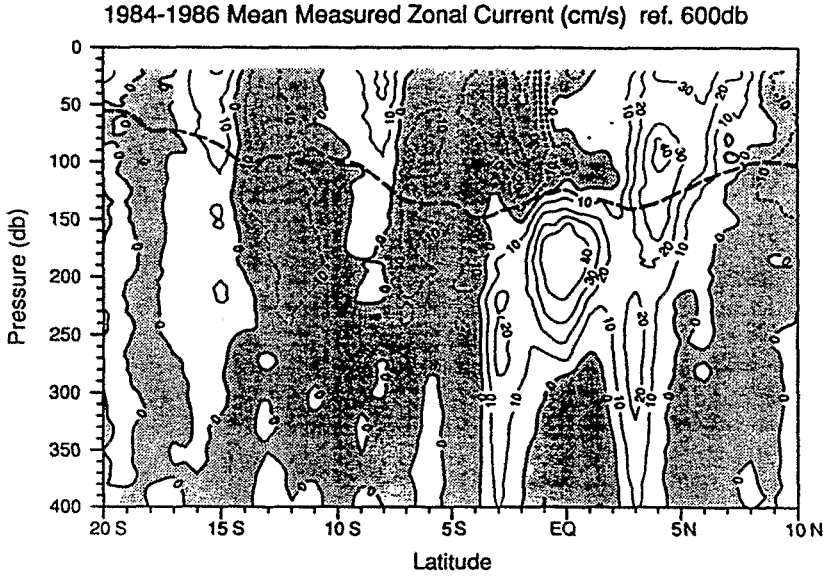

Fig. 8. Reference section of measured zonal current at 165°E, calculated from the 1984–1986 SURTROPAC cruises. The contour interval is 10 cm s^{-1}, and shaded areas denote westward flows. Currents are relative to 600 dbar. The mean 23.5 σ_t isopycnal is denoted by the heavy dashed line.

include 10°N by September 1987, and then returned southward to 15°S. Easterlies returned south of the equator in April 1988. The 1988 northern hemisphere winter trades were stronger than normal and extended south across the equator to join the southern hemisphere easterly maximum in August–September.

These patterns of wind stress at 165°E were part of the much larger scale evolution of the low-latitude wind field in 1986–1988 (Figure 9*b*). From January 1984 to June 1986, strong trade winds (above 30 m^2 s^{-2}) extended from about 120°W to 170°E, while westerly winds were confined west of 160°E. The trades then began to retreat eastward. Westerlies extended from Indonesia to 170°W in December 1986, with maximum strength between 160°E and the date line. Monthly wind maps confirm that this band of westerlies moved southward to cause the secondary southern hemisphere maximum observed at 165°E in February 1987, while westerlies weakened on the equator. The zone of strongest trades continued to shrink eastward until July–August 1987, when it began to expand back toward the west. After the November 1987 to March 1988 monsoon period of westerlies, the trades expanded westward to encompass nearly the breadth of the Pacific. Strong easterlies occurred west of 165°E several times in 1988, a year when the average eastward stress west of 170°E was stronger than in any other year of the period under study. Late in 1988, the easterlies were replaced by more typical weak monsoon westerlies in the far western Pacific.

Monthly anomalies of SST near the equator at 155°E, 160°W, and 100°W were compiled in the atlas of *Delcroix*

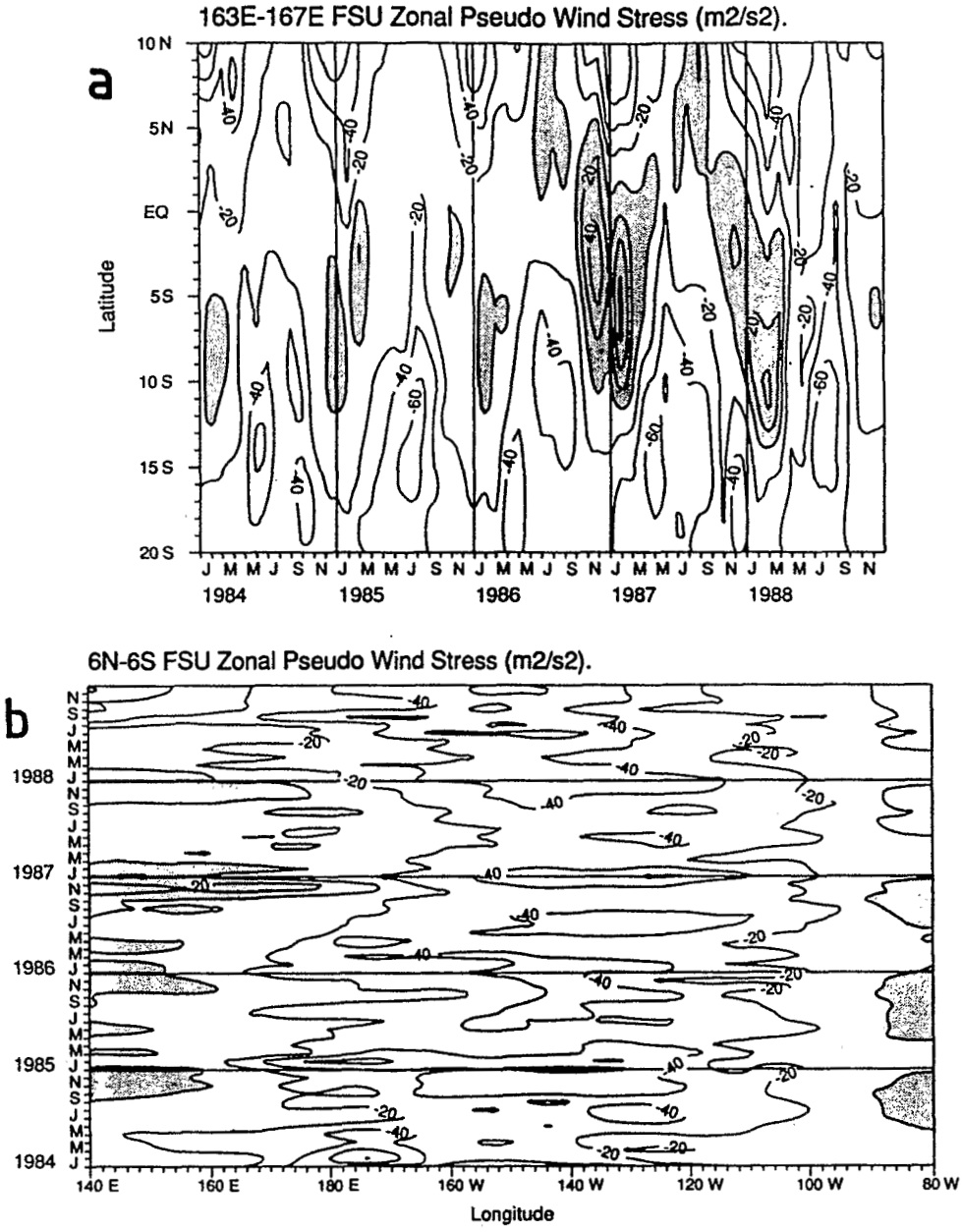

Fig. 9. Zonal pseudo wind stress ($m^2\ s^{-2}$), averaged from (*a*) 164°E to 166°E and (*b*) 6°N to 6°S. Shaded areas denote westerly winds.

and Masia [1990] (Figure 10). SST in the eastern Pacific rose rapidly in the first half of 1986 and then again in January–February 1987, leading to a maximum warm anomaly in the first quarter of 1987 (Figure 10). Warm temperatures persisted through October–November 1987, whereupon SST anomalies dropped to a notable minimum in June–July 1988. In the eastern equatorial Pacific then, the SST evolution was qualitatively similar to the *Rasmusson and Carpenter* [1982] SST composites at Puerto Chicama (7°S, 80°W) and along the Peru coast (see their Figure 8). Relative to the SST composite, however, the 1986–1987 event began 3–4 months earlier and lasted 18 months rather than 12 months.

At 160°W the warmest SST anomalies occurred during August–September 1987. This was about 6 months after the coastal SST anomaly peak, as in the *Rasmusson and Carpenter* [1982] composite. Along 155°E the SST variations were small (Figure 10) and approached the accuracy of bucket SST measurements. Nevertheless, we believe the cold SST anomaly observed in September 1987 is real; it exceeds the 0.2°–0.3°C uncertainty in bucket measurements.

The warm SST anomalies of the El Niño in the eastern and central Pacific were followed by cold anomalies in 1988. We will show in section 5 that this La Niña condition, with strong equatorial upwelling, was observed as far west as 165°E.

The ENSO signal in surface dynamic height in the western equatorial Pacific (Figure 11) was more prominent than the SST signal. Near the equator, 155°E, the dynamic height was lower in 1984 than in 1985; the change was of the order of 15 dyn cm between early 1984 and a pair of positive

extrema in May 1985 and April 1986. Thereafter, dynamic height dropped sharply by 26 dyn cm to a minimum during August–September 1987, about 3 months after the minimum SOI (Figure 4), then rose to a positive anomaly of 12 dyn cm in March 1989, several months after the peak in SOI. By the end of 1989, the height anomaly returned to near zero.

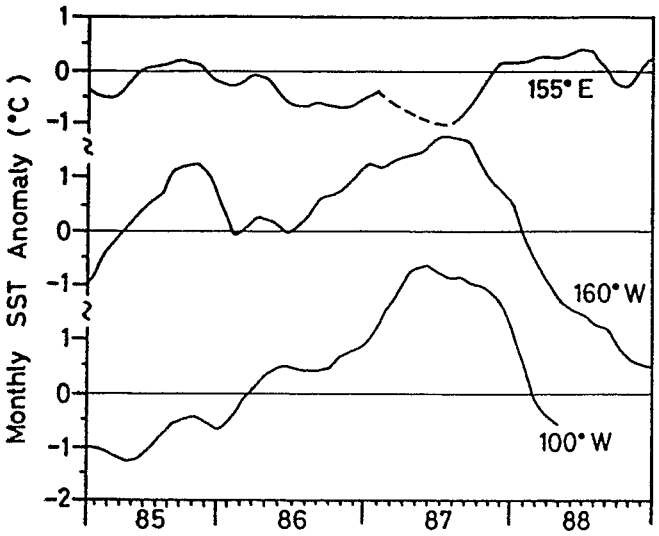

Fig. 10. Monthly sea surface temperature anomalies at the equator, for the 155°E, 160°W, and 100°W longitudes. The dashed line at 155°E denotes interpolated values.

The depth of the thermocline (Figure 11) roughly mirrored the dynamic height anomaly, but there were also major changes in thermocline thickness. From January 1984 to mid-1986, the equatorial thermocline near 155°E deepened by 45 m. Over the next 12 months, isotherms rose, recovering the earlier drop. The lowest SST (Figure 10) occurred during this period of shallow thermocline. The shoaling of isotherms was accompanied by a weakening of the thermocline (isotherms above 14°C spread apart). The thickness of the warm pool (the surface layer with $T > 28$°C) was reduced to 50 m during most of 1987, compared with about 80 m in 1984–1986. In late 1987 through early 1989, the thermocline deepened and sharpened; after the abrupt drop of isotherms below 20°C in August–November 1987, warmer isotherms descended faster than colder ones, compressing the thermocline. The 20°C isotherm reached a maximum depth of 200 m in March 1989, when the warm pool was 120 m thick. The trend during the remainder of 1989 was roughly toward the "normal" pre-1987 conditions, although the thermocline remained sharper and the warm pool thicker than during most of 1984–1986.

A broad view of the net zonal surface flow across 165°E is provided by tide gauge data. On average, absolute sea level

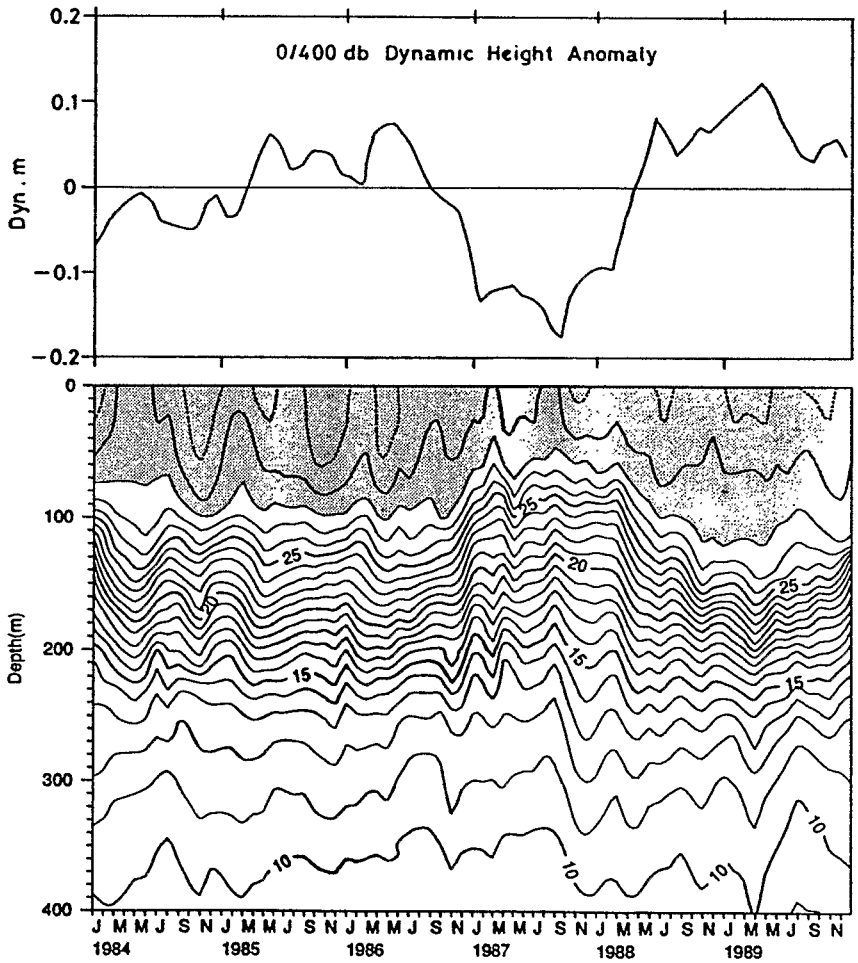

Fig. 11. (Top) Monthly variations of the 0/400 dbar dynamic height relative to the 1984–1986 mean value (1.26 dynamic meters), computed from XBT profiles in the region 2°S to 2°N, 145°–160°E. (Bottom) Corresponding isotherm depths. Areas with temperature greater than 28°C are shaded.

slopes down to the north from around 10°S across the equator to 10°N (Figure 5), in geostrophic balance with the SEC and NECC. Time series of the net height differences between 10°N and the equator, and between 10°S and the equator, may therefore be thought of as crude indices of net zonal transport of surface waters [e.g., *Wyrtki*, 1974]. For most of 1984, 1985, and the first half of 1986, net westward flow is inferred for the region south of the equator (Figure 2) while net eastward motion is indicated to the north; referenced sea level was nearly always higher at Honiara than at Nauru, and lower at Kwajalein than at the equator. There is the suggestion of a seasonal cycle in the records with strongest SEC early in the calendar year when the NECC is weak, followed by a period of enhanced NECC in midyear to boreal fall. In the latter half of 1986 this pattern was broken; sea level at Honiara and Kwajalein fell, the former to levels comparable to the equatorial station, while Kwajalein attained local minimum values. In terms of the net geostrophic surface flow, these changes correspond to enhanced eastward motion. Early in 1987, sea level near the equator began falling as well, while heights north of the equator rose. The middle of 1987 was thus characterized by little large-scale relief in the surface topography along 165°E, implying weak net zonal flow. Large-scale meridional sea level gradients returned in the last quarter of 1987, first with a fall in level at Kwajalein from September through December, followed by a sharp increase at Honiara early in 1988. The height difference between Honiara and the equator persisted through 1988 but that between Nauru and Kwajalein did not. In fact, the sea level difference north of the equator was minimal for much of 1988. The interpretation of these gradients in terms of geostrophic flow suggests a preponderance of westward surface flow. Finally, late in 1988, an indication of net eastward surface flow north of the equator returned when Kwajalein sea level fell below that at Nauru.

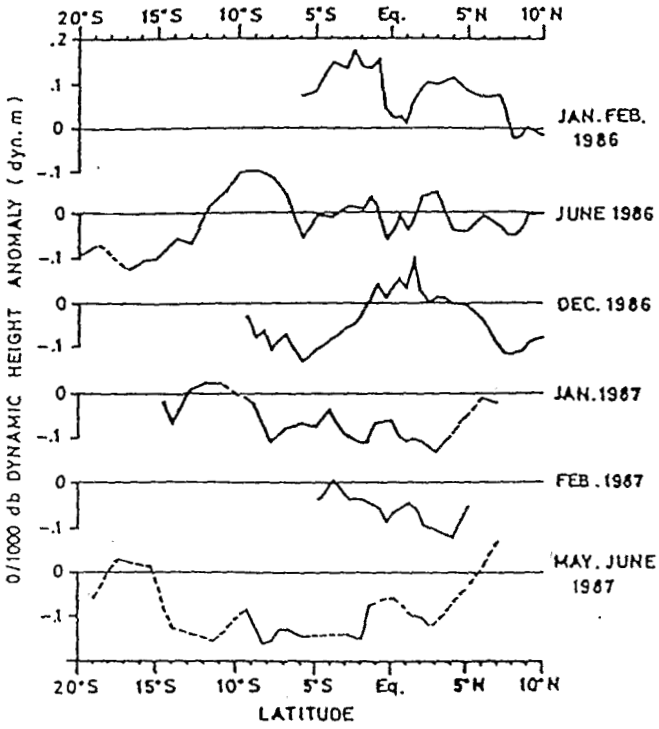

Fig. 12. Sections of 0/1000 dbar dynamic height anomalies (dynamic meters) at 165°E, relative to the reference 1984–1986 section (see Figure 5). Dashed lines appear between values separated by more than 2° latitude. Note that 0/500 dbar dynamic height anomaly is reported for the February 1987 cruise. The sections are presented for the January–February 1986 to May–June 1987 cruises.

5. Chronology of the Hydrography and Circulation at 165°E

With this overview of the large-scale oceanic and atmospheric variability in hand, we now turn to a detailed description of the changes seen at 165°E as revealed by the 15 cruises between 1986 and 1988.

5.1. *The Pre-El Niño Period (1984 to Mid-1986)*

Wyrtki [1975] proposed that the El Niño cycle has three definite phases that can be seen in the western Pacific as an accumulation of warm water before the El Niño, release of the warm water to the east during the event, and subsequent recovery. The release and recovery phases are obvious for the 1986–1987 event in both the XBT temperature profiles around 155°E and the dynamic heights derived from them (Figure 11). The buildup phase is not obvious in the complex temperature record but is suggested by the rising trend in dynamic height during 1984 and early 1985. Meridional profiles of 0/1000 dbar dynamic height anomalies on 165°E from the three cruises in 1986, however, show no evidence of a buildup (Figure 12). This is not surprising; many more sections would be needed to distinguish a trend amid the many energetic, high-frequency events [e.g., *Toole et al.*, 1988, Figure 5]. Better resolved dynamic height time series from moorings at 2°S, 165°E [*Hénin*, 1989] and 0°, 165°E [*McPhaden et al.*, 1990] did show an increase of about 12 dyn cm in sea level from mid-1985 (which was the beginning of the 2°S time series) to April–May 1986 when the trade winds started to decrease. We thus conclude that a buildup of warm surface waters probably occurred prior to the 1986–1987 El Niño, but with smaller amplitude than in *Wyrtki's* [1985] scenario. The absence of a corresponding trend in SOI (Figure 4), which was remarkably flat during this period, indicates that the buildup was caused by ocean dynamics and/or local winds, not by the basin-wide winds.

5.2. *El Niño Onset Period (August to December 1986)*

The anomalous westerlies associated with El Niño did not appear until mid-1986 (Figure 9; section 4); the thermohaline fields and circulation pattern at 165°E in June 1986 (SURTROPAC 6 cruise) did not differ significantly from climatology (Figures 12, 3). However, by December 1986 (USPRC 2 cruise), westerly winds had become strong and an intense eastward surface current had formed on the equator (Figure 13). For convenience we will call this flow the Eastward Equatorial Current (EEC). Approximately centered on the equator, the EEC was about 400 km wide and 125 m deep. Its maximum speed exceeded 1 m s^{-1}, and the associated eastward transport above 23.5 σ_t within 2° of the equator was 46×10^6 m^3 s^{-1}. Consistent with a geostrophic balance of this strong eastward surface flow, the 0/1000 dynamic height distribution was peaked at the equator. Relative to the average height field (and SURTROPAC 6), sea level was elevated by 4 dyn cm at the equator (Figure 12).

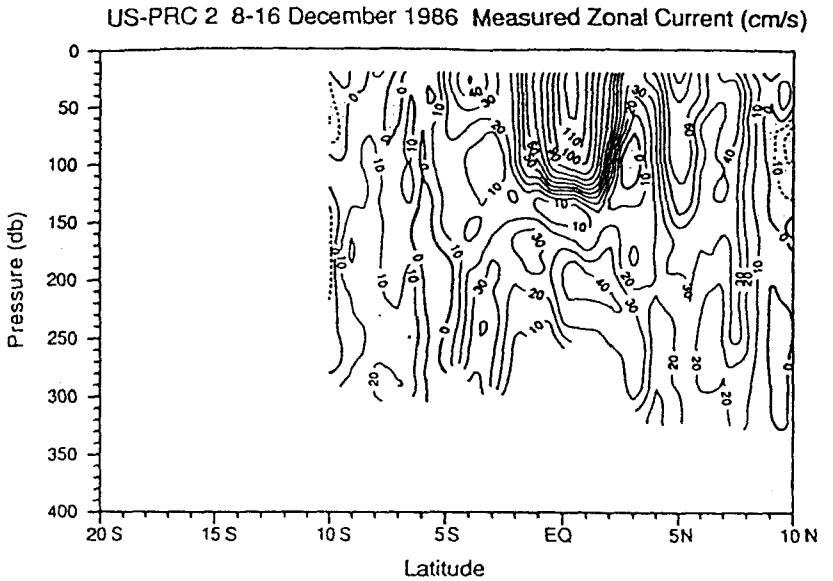

Fig. 13. Section of absolute zonal current at 165°E during December 8–16, 1986 (US-PRC 2 cruise). Contour intervals are 10 cm s^{-1}. Shaded areas denote westward flows.

We believe the EEC was the result of strong westerly wind stress events at and west of 165°E in November and December 1986. During US-PRC cruise 2, winds with a westerly component were observed from 5°N to the southern end of the section at 9.5°S; the vector-averaged eastward wind speed within 5° of the equator was 8 m s^{-1}, with speeds south of the equator twice as large as those to the north. The time series plots of Figure 9 suggest westerly winds also occurred prior to this cruise. Despite the complicated time history of the winds, the scales and strength of the December 1986 EEC are strongly reminiscent of the analytical and numerical model results of the equatorial ocean's response to the sudden onset of winds [*Yoshida*, 1959; *Philander*, 1979; *Philander and Pacanowski*, 1980]. Also consistent with model results, subsequent satellite sea level observations [*Miller et al.*, 1988] revealed an eastward propagation of elevated equatorial sea level with characteristics of a first vertical mode Kelvin wave [*Delcroix et al.*, 1991].

Currents in December 1986 were strongly eastward over most of the latitude range 5°S to 9°N, not just near the equator. Peak speed in the NECC exceeded 80 cm s^{-1}, and the upper layer transport over the latitude range 5°S to 9°N was 86×10^6 m^3 s^{-1} (Figure 3). Concurrent with the off-equator eastward flows were pronounced dynamic height anomalies, again in the sense consistent with geostrophic balance (Figure 12). Negative anomaly extrema were found around 7°S and 7°N; the latter is near the average location of the sea level trough between the NECC and NEC. The southern anomaly extremum represents the absence of the dynamic height ridge normally found between the SEC and SECC (Figure 5). Maps of the Ekman pumping velocity [*Eldin and Delcroix*, 1989] suggest that these features were locally forced; pronounced areas of anomalous upwelling were inferred equatorward of 10°S and 8°N in October–December.

In contrast with the surface currents, the subsurface currents in December 1986 were near average. The volume transports of the EUC, NSCC, and SSCC were within 75% of the 1984–1986 mean (Table 2). Changes in the deeper density field between July and December 1986 were relatively small also. While the thermocline shoaled between December and July (leading to lower dynamic heights), within 800 km of the equator isopycnals below about 300 m deepened, but by only 50 m or less. The largest displacements were found off the equator.

5.3. *The El Niño Mature Phase (January to October 1987)*

During this period, the ocean-atmosphere system exhibited many characteristics of the mature stage of El Niño: (1) the SOI fell to a minimum value around April–June 1987 (Figure 4), (2) frequent outbreaks of westerly winds occurred on the equator, and (3) the thermocline in the western Pacific was shallow [*Eldin and Delcroix*, 1989] and surface dynamic heights were depressed (Figure 11).

Alternating zonal wind stress near the equator during the first half of 1987 led to frequent reversals of the surface current but little change in the subsurface currents (Table 2). Direct measurements from the January 1987 cruise (SURTROPAC 7) [*Eldin*, 1988] revealed a significantly weakened EEC in the upper 100 m (5.1×10^6 m^3 s^{-1}), and most of the equatorial doming in dynamic height anomaly that was seen the previous month was gone (Figure 12). By early February 1987 (JENEX 1), after 1 month of easterlies, the equatorial surface current was westward and surface dynamic height at the equator was lower than at 2°N and 2°S. Eastward equatorial surface flow began again in early May 1987, detected by the 165°E equatorial current meter mooring [*McPhaden et al.*, 1990], and a corresponding equatorial peak in dynamic height anomaly was found in late May and early June (SAGA 2; Figure 12). Throughout this period, surface dynamic height within about 10° of the equator was 10–20 dyn cm below the reference field, consistent with a net shift of warm water from the western to the central and eastern Pacific during the El Niño onset. This shift is corroborated by the observation that dynamic height of the surface

relative to 250 dbar was more than 10 dyn cm higher than normal on the equator at 140°W and 110°W from mid-1986 through the end of 1987 [*McPhaden and Hayes*, 1990].

The July and September 1987 cruises (SURTROPAC 8, TEW 3, PROPPAC 1) occurred during a period when the SOI was returning to zero. The FSU wind field analysis shows easterly wind, close to climatology, south of 2°N but unusual westerlies north of this latitude (Figure 9). Direct wind measurements, however, conflict with this analysis. Westerly winds were observed at the equatorial mooring on 165°E [*McPhaden et al.*, 1990] through mid-October 1987 and were particularly strong in June and July. Similarly, on SURTROPAC 8 during July 9–12, 1987, southwest winds greater than 10 m s^{-1} were measured between 4°S and 3°N.

Of particular interest in the cruise data from this period are the zonal current distributions. During the July–September cruises (SURTROPAC 8, Figure 14; TEW 3, Figure 15; and PROPPAC 1, Figure 16), anomalous eastward flow was everywhere present in the upper 100 m between about 5°S and 6°N. Net transport of the EEC was 30.2×10^6 m^3 s^{-1}, 44.7×10^6 m^3 s^{-1}, and 22.3×10^6 m^3 s^{-1} for these three cruises, respectively. (Note that the SURTROPAC 8 transport estimate required linear interpolation between missing stations). Marked changes of the thermohaline structure were also observed. These included (1) the signature of equatorial downwelling in the meridional distributions of upper ocean temperature, density, and dynamic height [*Eldin*, 1989; *Blanchot et al.*, 1987], (2) a continued

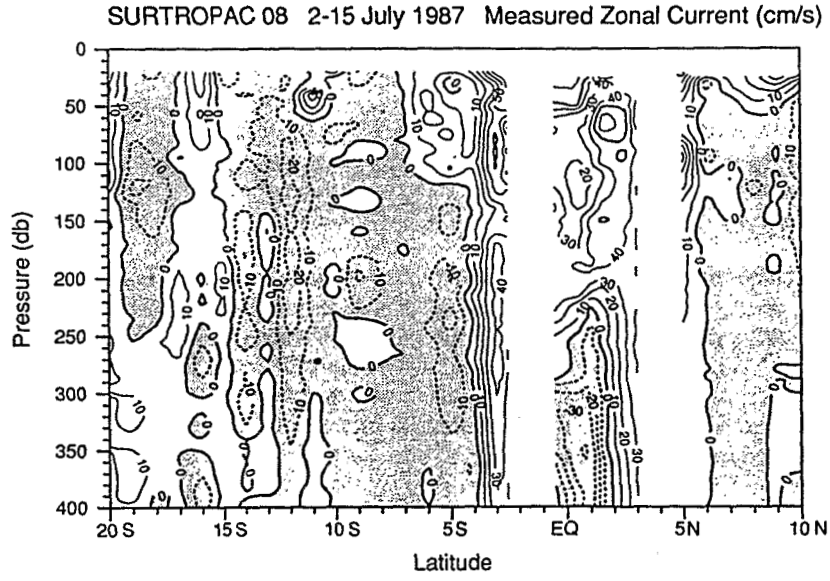

Fig. 14. Section of zonal current (relative to 600 dbar) at 165°E during July 2–15, 1987 (SURTROPAC 8 cruise). Contour intervals are 10 cm s^{-1}. Shaded areas denote westward flows.

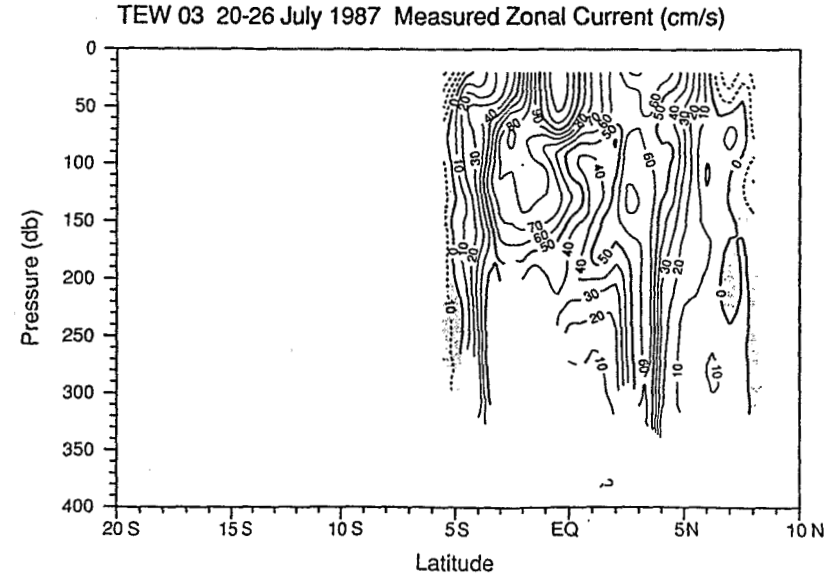

Fig. 15. Section of absolute zonal current at 165°E during July 20–26, 1987 (TEW 3 cruise). Contour intervals are 10 cm s^{-1}. Shaded areas denote westward flows.

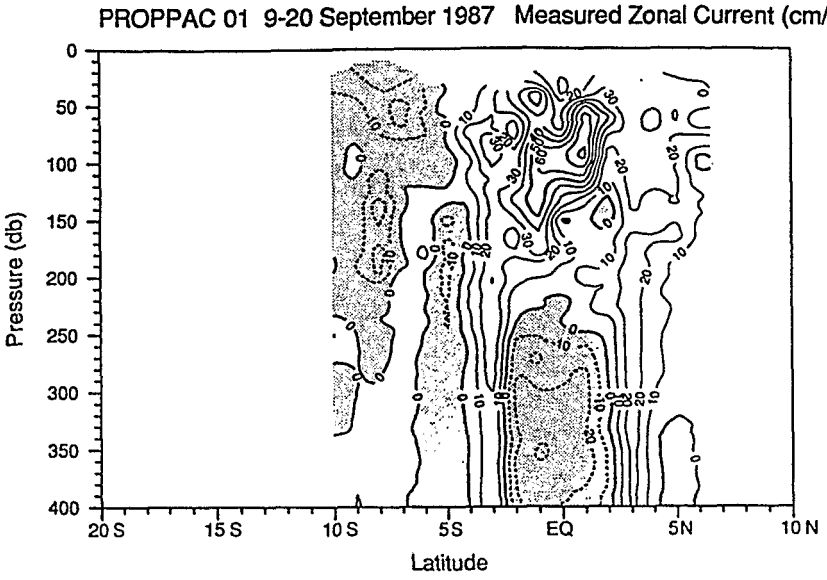

Fig. 16. Section of zonal current (relative to 600 dbar) at 165°E during September 9–20, 1987 (PROPPAC 1 cruise). Contour intervals are 10 cm s^{-1}. Shaded areas denote westward flows.

0- to 50-m shoaling of the 20°C isotherm in the equatorial and [*Eldin and Delcroix*, 1989], and (3) very fresh water less than 34.50 psu) in the upper 60 m extending from 9°S o 10°N (from the approximate southern limit of the mean ECC to the northern limit of the mean NECC). Aspects of ıe unusual vertical salinity distribution during this period ill be detailed in section 6.

Both local and remote forcings appear responsible for the redominantly eastward currents and the diffuse, shallow ıermocline. The intense but shallow EEC seen in late July TEW 3; Figure 15), with a maximum speed greater than .1 m s^{-1} at 0.5°S, looks like a response to the local west-ly winds, as was the deeper EEC of the El Niño onset in ecember 1986 (US-PRC 2; Figure 13). On the other hand, ıe September 1987 cruise was neither preceded by nor un-ertaken during a westerly wind episode at 165°E, yet an EC was still present.

Delcroix et al. [1991] suggested that remote forcing in ıe form of an upwelling equatorial Rossby wave con-ibuted much to the eastward near-equatorial flows ob-:rved at 165°E in July–September 1987. These authors lentified a westward propagating (mean phase speed = 02 ± 0.37 m s^{-1}) sea level signal in the Geosat altimetric ata set which had the meridional structure of a first merid-nal mode equatorially trapped Rossby wave. This fea-ıre originated in the eastern Pacific and reached 165°E in ly–September 1987. *Delcroix et al.* [1991] noted that the owelling Rossby wave would cause strong eastward equa-rial flow anomalies and westward (and somewhat weaker) omalies at higher latitudes, decreasing the transports of th the NECC and SECC (see their Figure 12).

The dynamic height and velocity fields observed along 5°E during July–September 1987 are consistent with the ossby wave inferred from Geosat sea level. The anoma-s of the meridional 0/1000 dbar dynamic height struc-ıres (alias for sea levels) observed during July–September 87 resemble the theoretical shape $h(y)$ of sea level for a st baroclinic, first meridional mode Rossby wave (Fig-ure 17*a*). The least squares fits of $h(y)$ to the observed anomalies of 0/1000 dynamic heights give values $h(0)$ close to −10 dyn cm for each of the three cruises (−8.2 for SUR-TROPAC 8, 10°N to 10°S; −10.6 for TEW 3, 8°N to 5.5°S; and −9.1 for PROPPAC 1, 6°N to 10°S). At the equator, the geostrophic current corresponding to $h(0) = -10$ dyn cm is nearly 1 m s^{-1}. The observed 50- to 100-m current anomalies for the three cruises are only about half this speed at the equator, but poleward of 1°–2° they agree better with the theoretical Rossby wave (Figure 17*b*).

Given that the meridional structure of the shallow current and dynamic height anomalies roughly resembles a Rossby wave, and that both the meridional scale and the zonal propagation speed of the wave suggest the vertical structure of the first baroclinic mode [*Delcroix et al.*, 1991], it is reasonable to ask whether the observed dynamic height and current anomalies are indeed first baroclinic mode. We find that they are not quite; both the current and the dynamic height anomalies, averaged from 5°N to 5°S, are essentially confined to the top 200 m, whereas the first baroclinic mode at 200 m still has more than a third of its surface amplitude (Figure 18).

While the SOI, and thus the large-scale atmospheric circulation, moved still closer to normal conditions in boreal fall 1987, the western Pacific Ocean entered the peak phase of El Niño. The October 1987 cruise (US-PRC 3) sampled highly perturbed velocity and thermohaline fields along 165°E (Figure 19). Westward flow was found almost everywhere between 3°S and 2°N in the upper 300 m of the water column; the EUC had disappeared. *McPhaden et al.* [1990] demonstrated that this condition, which persisted for about 1 month before eastward subsurface flow returned, was associated with a reversal of the zonal pressure gradient (P_x) at the depths of the EUC. This reversal must have been due to propagating equatorial waves; it occurred during a period of light winds in the western Pacific, about a year after the strong westerlies of the El Niño onset.

With only four zonal sections available to *McPhaden et*

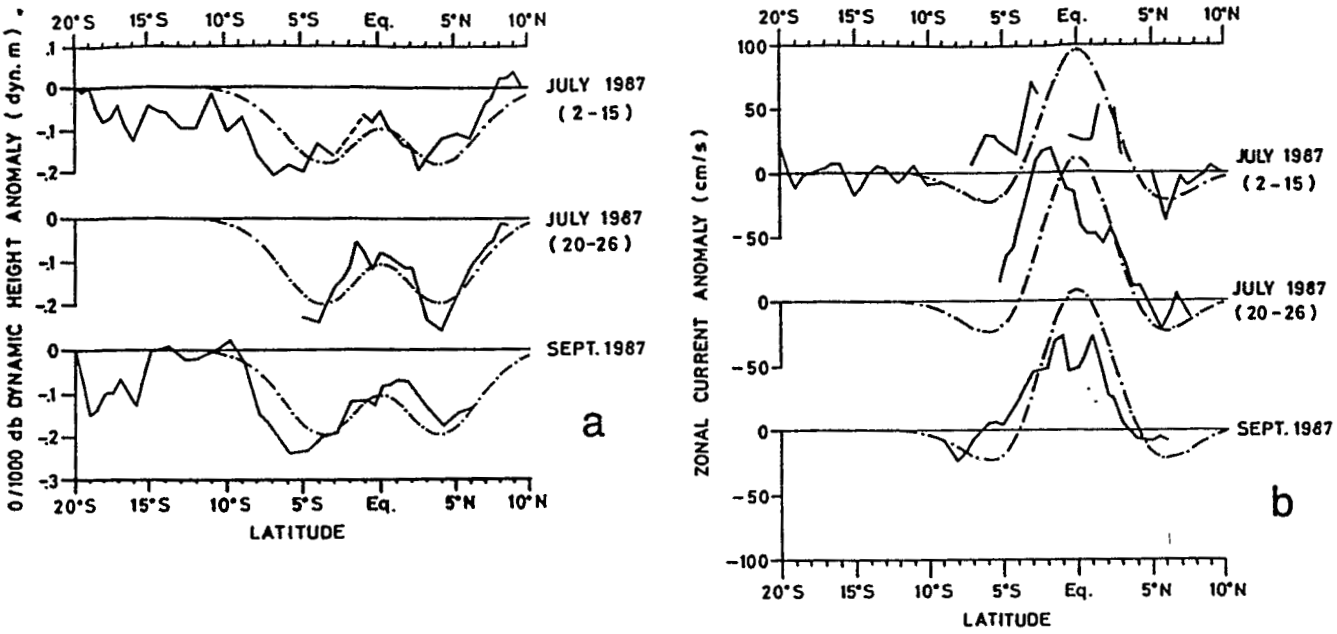

Fig. 17. Sections of (*a*) 0/1000 dbar dynamic height anomalies and (*b*) 50- to 100-m average current anomalies at 165°E, relative to the reference 1984–1986 section. Dot-dashed lines are the 10°N to 10°S least squares fits of the anomalies to the theoretical sea level signature of a first baroclinic ($c = 2.8$ m s^{-1}) [*Delcroix et al.*, 1991], first meridional mode upwelling equatorial Rossby wave. The sections are presented for the July to September 1987 cruises.

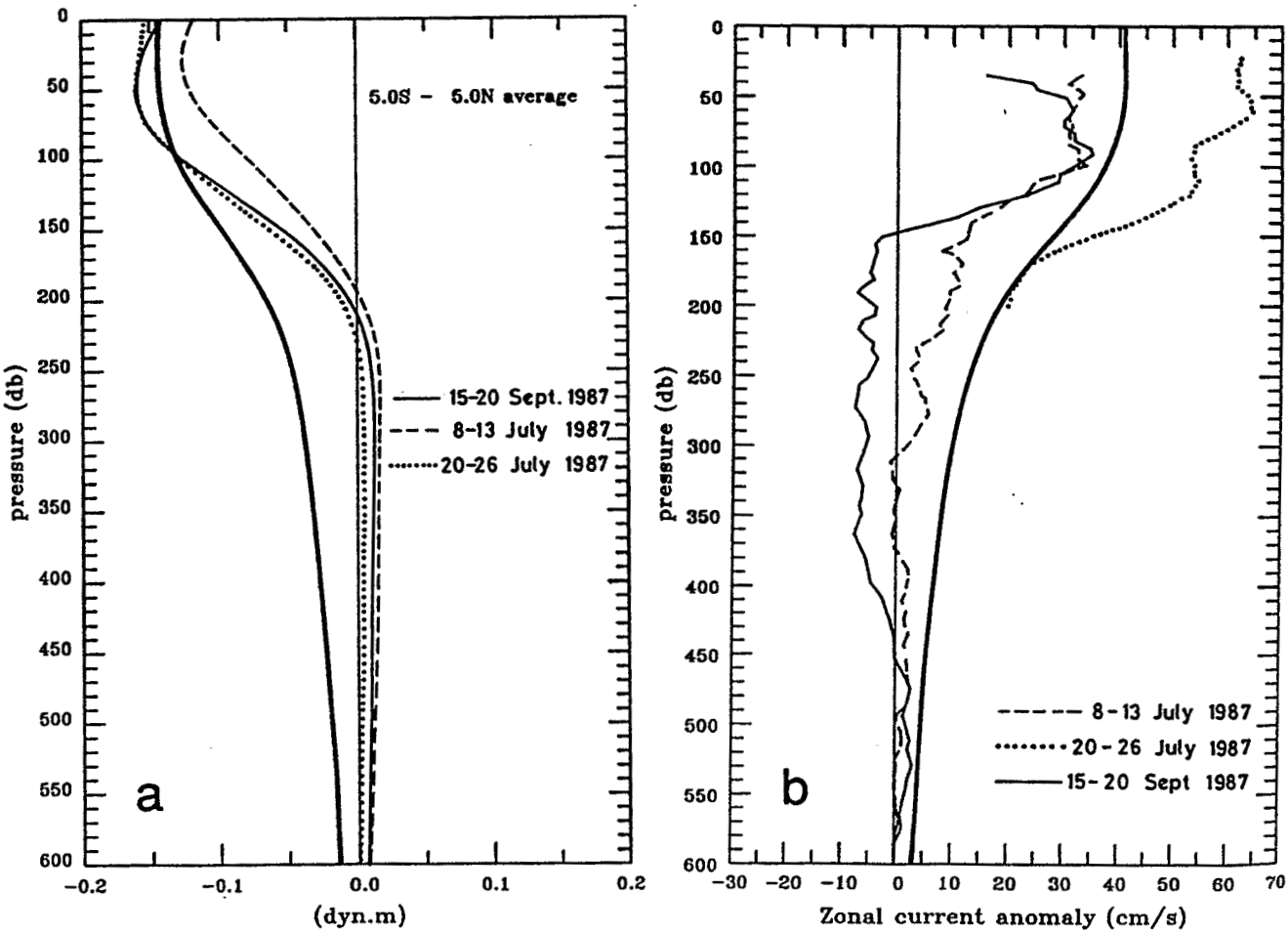

Fig. 18. Vertical distributions of 5°N to 5°S averaged (*a*) dynamic height anomalies (0/1000 dbar) and (*b*) zonal velocity anomalies at 165°E, relative to the reference 1984–1986 section. The theoretical first baroclinic mode is included for comparison (heavy line). The distributions are presented for the July to September 1987 cruises.

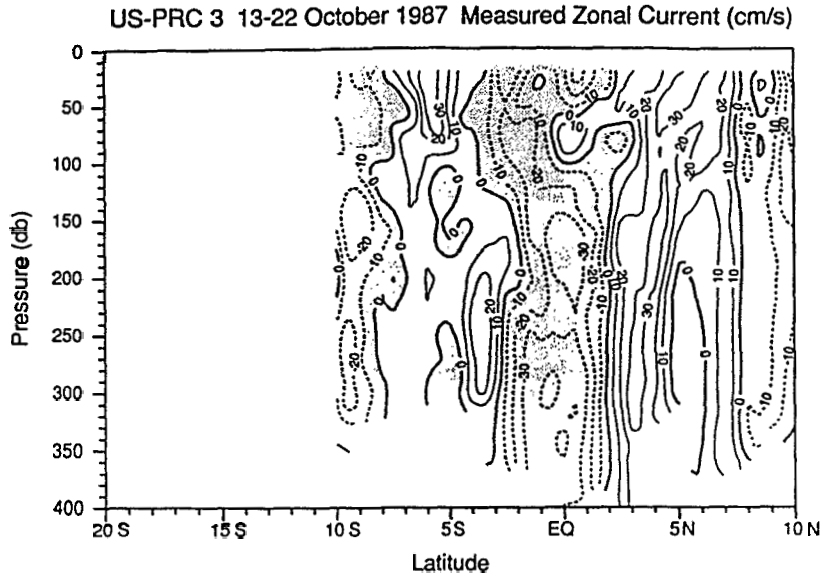

Fig. 19. Section of absolute zonal current at 165°E during October 13–22, 1987 (US-PRC 3 cruise). Contour intervals are 10 cm s^{-1}. Shaded areas denote westward flows.

al. [1990], the phase relationship between the EUC and P_x could not be determined. It can be explored, however, using estimates of the sea level slope along the equator, assuming P_x does not change sign between the surface and the EUC core. This assumption cannot be demonstrated from our data set, but it was verified with data from four equatorial US-PRC sections from 140°–165°E [*McPhaden et al.*, 1990], and from various other measurements of P_x in the three tropical oceans [see *Weisberg and Weingartner*, 1986].

We used the sea level records from the islands of Kapingamarangi and Christmas to estimate P_x at the equator; these islands bracket the region of interest (see Figure 1) and have a 10-year common record. The climatological 0/500 dbar dynamic height difference between Kapingamarangi and Christmas is 16 cm. Assuming this dynamic height difference is also the mean sea level difference, we found three periods in the 10-year record when the surface P_x reversed: first from late July 1982 to early January 1983 (170 days), second from mid-December 1986 to late January 1987 (45 days), and third from mid-July to early October 1987 (80 days). The second period was associated with weak EUC velocity [*McPhaden et al.*, 1990]; the EUC core disappeared about 2 months after the beginning of the first and third periods [*Firing et al.*, 1983; *Tournier*, 1989; *McPhaden et al.*, 1990]. From this we would conclude that the time lag between the reversal of P_x and the disappearance of the EUC core is about 2 months.

Indication of a longer-term reduction of the zonal pressure gradient at thermocline depths in 1987 was seen in the meridional distribution of salinity along 165°E. The meridional salinity gradient at the equator within the subtropical high-salinity core ($24 < \sigma_t < 25.5$) was reduced by half in late 1987 as compared with the average conditions. This gradient is presumably maintained in the face of lateral mixing by equatorward geostrophic convergence supported by the eastward pressure gradient force characteristic of the equatorial Pacific. From the reduced meridional salinity gradient observed in late 1987 we therefore infer a weakened zonal pressure gradient.

As would be expected from the absence of eastward equatorial flow, there was no doming of isopycnals about the equator in October 1987; the stratification from 25- to 225-m depth was comparable at all stations between 3°N

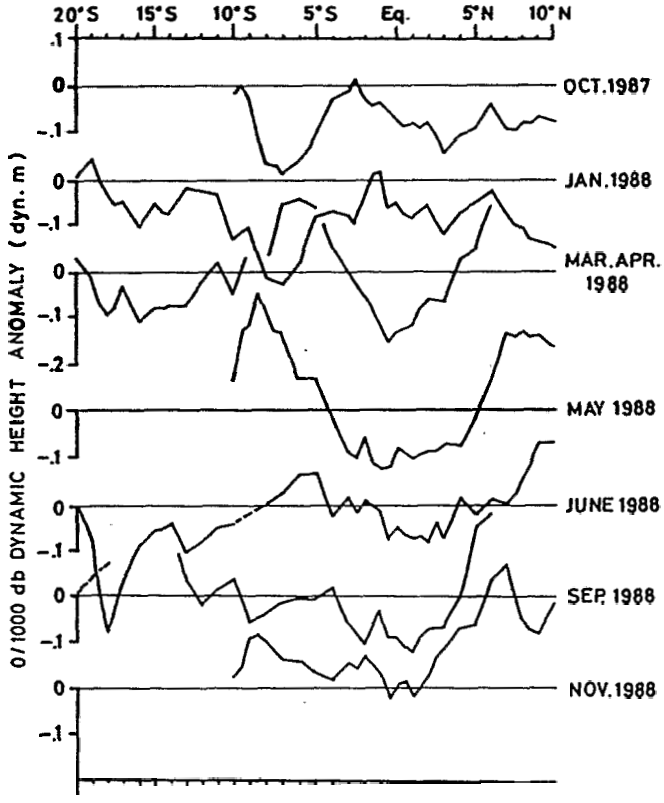

and 1.5°S. Surface dynamic heights near the equator averaged 8–10 dyn cm below the reference field, chiefly because the pycnocline (represented by $\sigma_t = 23.5$) was 50 m shallower than average. Deeper isopycnals were not displaced far from their mean levels; below 400 m, density surfaces within 200 km of the equator averaged 20 m deeper than in the 1984–1986 mean section. Consequently, the meridional density gradients associated with the NSCC and SSCC were relatively unchanged at the time of EUC disappearance. Direct current measurements also showed the NSCC and the SSCC to be similar to the reference field.

Evidence that the arrival of a Rossby wave caused the return of the SEC in October 1987 is suggestive but incomplete. Local forcing was clearly weak; the 0°, 165°E mooring record [*McPhaden et al.*, 1990] shows that the SEC appeared rapidly in mid-October when the local winds were near zero (Figure 9). The Geosat sea level data analysis of *Delcroix et al.* [1991] suggested that a first baroclinic, first meridional mode downwelling equatorial Rossby wave may have reached 165°E in October 1987. Such a wave would induce an equatorially trapped westward flow bounded by eastward currents which would reinforce the NECC and SECC. The return of the SEC, as well as the strong SECC observed in October 1987, is qualitatively consistent with this remote forcing explanation, but comparisons between dynamic height and zonal current anomalies and the corresponding structures of the downwelling Rossby wave (not shown) are in quantitative disagreement, mainly in the NECC. This may simply indicate that the hypothetical Rossby wave is only one of several significant phenomena. Perhaps, also, at this stage in the event all memory of the mean currents has been lost, so that anomalies from the mean are no longer the appropriate fields to compare with the theoretical wave fields.

5.4. *The La Niña Period (February to October 1988)*

Basin-wide atmospheric and oceanic indices concurred in suggesting continued return toward normal conditions from November 1987 to February 1988. The SOI and eastern Pacific SST anomalies crossed zero (SOI from negative to positive values, SST from positive to negative) around Febru ary 1988 (Figures 4, 10). West of the date line, the win stress remained anomalously eastward, but with consider ably smaller amplitude than in the preceding year (Fig ure 9). Western Pacific surface dynamic height rose abruptl in this period and reached climatological levels in Marc 1988 (Figure 11) .

Surface dynamic height was still below average in Jan uary 1988 across nearly our full sampling interval of 20°S to 10°N (SURTROPAC 9; Figure 20), and strong eastwar countercurrents were present poleward of 5° latitude. Be ginning around February–March 1988, however, sea level of the equator began rising sharply while heights fell near th equator (Figure 2). This trend led to the pronounced bow in surface dynamic height about the equator observed or cruises during March–April and May 1988 (Figure 20). Remarkably, the dynamic height anomaly distributions with latitude sampled during March–April and May 1988 are nearly the mirror image of the distribution in November–December 1986 during El Niño onset (Figure 12).

The equatorial depression in surface heights was related to strong equatorial upwelling, caused by the expansion of the trade winds across the breadth of the Pacific in March 1988 (Figure 9). The signature of equatorial upwelling is clearly seen in most water mass property sections obtained in this period (Figure 21). The associated wind stress curl off the equator was favorable to a depression of the thermocline around 6°N and 6°S [*Eldin and Delcroix*, 1989], leading to dynamic height ridges at these latitudes. Equatorward of these ridges, surface dynamic height slopes were consistent with significant westward geostrophic flow in the SEC (Figure 22). The eastward countercurrents were shifted poleward as a result and weakened considerably. A similar weakening of the NECC was observed previously at the end of the 1982–1983 El Niño [*Meyers and Donguy*, 1984; *Tournier*, 1989].

The EUC, which had disappeared only 6 months earlier, was exceedingly well developed in boreal spring 1988 (Figure 22). Core speeds greater than 60 cm s^{-1} were observed during March–May 1988; the combined transport of

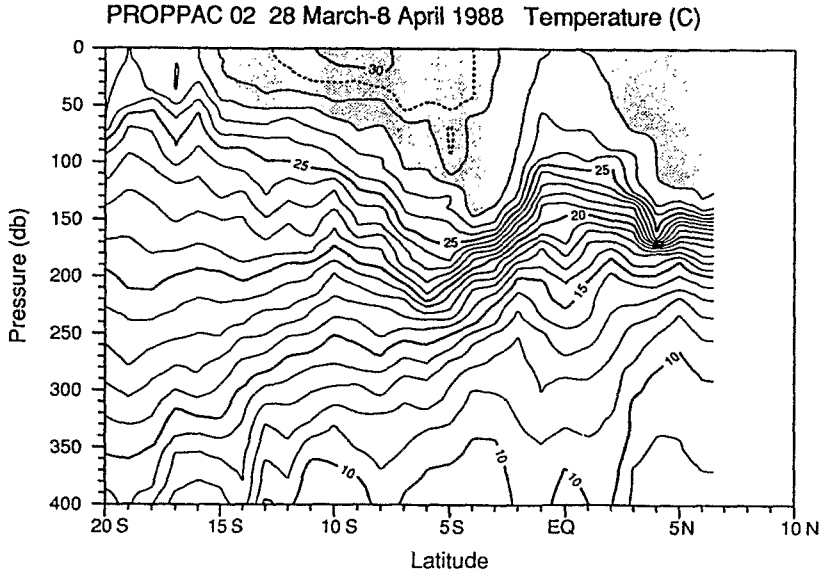

Fig. 21. Section of temperature at 165°E during March–April 1988 (PROPPAC 2). Note the strong equatorial upwelling characteristic of La Niña.

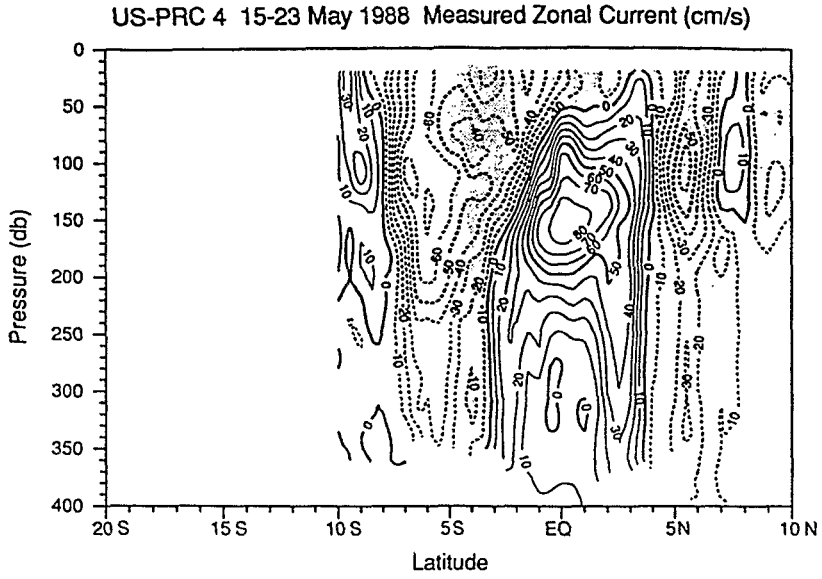

Fig. 22. Section of absolute zonal current at 165°E during 15–24 May 1988 (La Niña; US-PRC 4 cruise). Contour intervals are 10 cm s^{-1}. Shaded areas denote westward flows. The SEC and the EUC are strong, while the NECC is almost absent.

the EUC, NSCC, and SSCC exceeded 40×10^6 m^3 s^{-1}(Table 2). Consistent with the strong EUC, *McPhaden et al.* [1990] found an above-average eastward pressure gradient in the thermocline west of 165°E for this period. In addition, the meridional salinity gradient in the subtropical water sharpened in early 1988, which also suggests recovery of the zonal pressure gradient.

Although the eastward transport of the EUC was strong in early 1988, the net transport of warm water was strongly to the west on all cruises from March through November 1988, with the exception of SURTROPAC 10 in June (Figure 3). The island tide gauge data also suggest that anomalous net westward flow of surface waters continued during most of 1988 (Figure 2), restoring surface waters to the western Pacific. The bowl in surface dynamic height that was seen in spring 1988 weakened in the latter half of the year but remained identifiable on cruises in June, September, and November 1988 (Figure 12). Equatorial sea level gradually rose as surface waters were restored to the western Pacific so that by November 1988, 0/1000 dynamic heights were comparable to the reference values at the equator and exceeded them away from the equator. The 1986–1988 ENSO was ended.

6. Mixed Layer Structure

During the two WEPOCS cruises west of 155°E [*Lindstrom et al.*, 1987], a nearly isothermal, relatively deep surface layer was often found to contain a shallow isohaline layer. At the base of the isothermal layer, a second halocline was frequently observed [*Lukas and Lindstrom*, 1991]. Large differences between thermocline depth and halocline depth have also been found along 165°E [*Delcroix et al.*, 1987], similar to the WEPOCS region more than 1000 km to the west. There are many possible ways of defining mixed layer depths for these profiles; *Lukas and Lindstrom* [1991] chose gradient criteria to discriminate the top of the thermocline (0.05°C m^{-1}), the main halocline (0.02 psu m^{-1}), the intermediate halocline (0.01 psu m^{-1}), and the base of the density mixed layer (0.01 kg m^{-4}). For the present data set also, these gradient criteria proved superior to other criteria that were tested. We restricted our study to the latitude range 10°N to 10°S, for which we have the most data, and to depths greater than 10 m, neglecting the occasional near-surface (5–10 m) salinity gradients presumably caused by recent local rainfall.

Averaged over all cruises from 1984 to 1988, the isothermal layer depth, 60–100 m, exceeded the density mixed layer depth, 40–60 m, throughout the 10°S to 10°N range (Figure 23). The surface isohaline layer thickness was nearly identical to the density mixed layer thickness, confirming the importance of salinity stratification in governing the surface mixed layer depth.

Following the definition of *Lukas and Lindstrom* [1991], we consider the "barrier layer" as extending from the base of the density mixed layer to the top of the thermocline (that

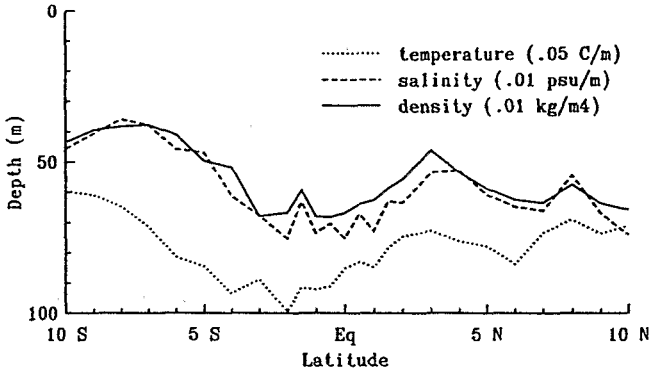

Fig. 23. Mean depths of the top of the thermocline (dotted line), the base of the isohaline layer (dashed line), and the base of the density mixed layer (solid line) along 165°E. The mean depths were computed over the 21 cruises reported in Table 1.

is, between the dotted and solid lines on Figure 23). The histogram of barrier layer thicknesses on 165°E for the period 1984–1988 is similar to the one calculated for the WEPOCS cruises. Barrier layer thickness estimates ranged from 0–80 m, with a mean of 24 m. Fully half of the observations contained a layer thicker than 10 m.

Lukas and Lindstrom [1991] suggest that the barrier layer is caused by the combination of heavy rainfall in the western Pacific, leading to a relatively fresh surface layer there, and the westward subsurface flow of more saline water subducted near the date line. They further show that the barrier layer is eroded from the top by wind mixing, particularly during strong westerly wind bursts. The importance of rainfall to the barrier layer at 165°E is confirmed by the variation of the layer with latitude. Well-developed barrier layers (>10 m thick) occurred most often at 5°S (80% of our observations) and 5°N (50%), which are the areas of maximum climatological precipitation (>3 m yr^{-1}) associated with the SPCZ and ITCZ [*Dorman and Bourke*, 1979, Figure 2; *Elliot and Reed*, 1984].

Major temporal and spatial variations of the barrier layer were associated with the time history of the winds, currents, and thermocline depth (Figure 24). From 1°N to 1°S, the barrier layer was virtually nonexistent in January and August 1984 because of equatorial upwelling [*Delcroix et al.*, 1987; Figures 3*a* and 3*b*]. The thickest barrier layers (40–80 m) were observed on the cruises between January 1985 and June 1986. In December 1986, the absence of the barrier layer coincided with the presence of the strong EEC (Figure 13). The barrier layer remained thin through 1987 despite strong precipitation (as deduced from cloud top temperature) [*Janoviak and Arkin*, 1991]. In the face of vertical mixing caused by winds and the EEC, the buoyancy forcing was apparently not sufficient to form a well-marked salinity mixed layer and hence a barrier layer. Another factor may have been the absence of the SEC on the equator (except in October 1987); the supply of saline water from the east was cut off. The barrier layer did thicken gradually to 30–40 m in early 1988 when the local winds weakened and the SEC returned to the equator. After March 1988, the return of strong trade winds (La Niña) at 165°E induced strong equatorial upwelling and wind mixing at the surface, both acting against development of a barrier layer. Indeed, layers were very thin or absent at these times.

The barrier layer south of the equator (4°–6°S) was similar in thickness to the equatorial barrier layer during 1985 and the first half of 1986, when both were thick, but it was not as thin as the equatorial layer at other times. This difference is presumably due to the meridional scale of the factors that inhibited barrier layer formation on the equator: equatorial upwelling, mixing by the EEC, and the absence of the SEC.

Within 4°–6°N, the barrier layer was about 20 m thick with a slight decrease from 1984 to 1987 and a maximum thickness (30–40 m) during the 1988 La Niña. During most of 1985 and 1986 the layer was much thinner north of the equator than elsewhere. This difference can probably be attributed to the NECC: it tilts the thermocline up to the north so that it is shallower at 5°N than at 5°S in the mean (Figure 6); and it advects relatively fresh water, compared with the saline water carried by the SEC (Figure 7). Increased westward flow of subducted water may have contributed to the barrier layer both north and south of the equator in 1988, when the SEC was unusually strong and the NECC weak. A second factor contributing to the thick barrier layers in 1988 may have been convergent surface circulation [*Lukas and Lindstrom*, 1991]; it was argued above that the development of dynamic height ridges around 5°N and 5°–10°S in 1988 (Figure 20) resulted from local downwelling driven by wind stress curl.

In summary, the 1°N to 1°S barrier layer was destroyed during episodes of eastward surface flow (commonly associated with strong westerly winds) and periods of equatorial upwelling driven by easterlies. Maximum layer thicknesses were found 4°–6° poleward of the equator when local wind stress curl drove downwelling. This supports the role of the near-surface oceanic circulation in barrier layer formation. The situation near the equator is complex, however. Layer formation is inhibited at times of strong easterlies by equatorial upwelling which works against zonal subduction. Westerlies force downwelling at the equator, but if the winds are too strong, barrier layers are inhibited by strong mixing and by the absence of westward advection of saline water by the SEC. Existence of the barrier layer appears to reflect a delicate balance among winds, precipitation, currents, and mixing.

7. DISCUSSION

Conditions in the western tropical Pacific Ocean during the 1986–1987 El Niño and the ensuing 1988 La Niña were observed more thoroughly than during any previous ENSO cycle. We have synthesized a picture of the oceanographic

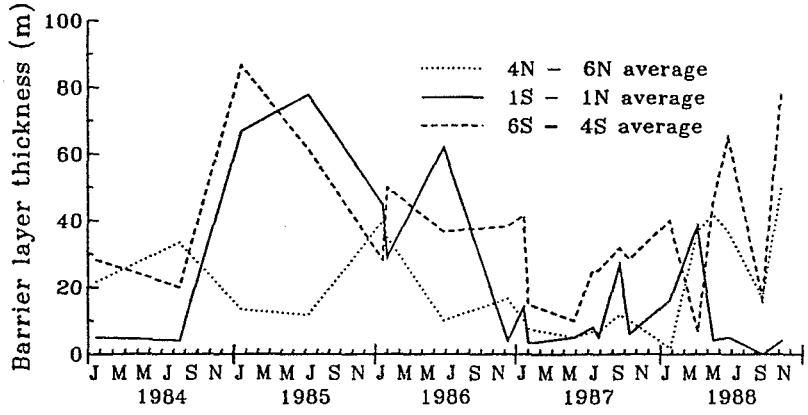

Fig. 24. Time series of the barrier layer thickness at 165°E for three different latitudinal bands.

changes at longitude 165°E from many types of measurements, the principal set being an unprecedented series of 21 oceanographic cruises along 165°E. These observations document striking variability in the zonal surface currents over this 2.5-year period. These currents, in turn, significantly altered the volume of warm surface waters in the western Pacific, as we will now demonstrate.

We derived a time series of western Pacific warm water volume anomaly (WWV) using the direct current measurements made on our cruises. For each cruise, an estimate of net zonal transport of waters above the 23.5 kg m^{-3} isopycnal was made for the band 10°N to 10°S. These transport estimates were then interpolated in time and integrated, giving us a hindcast WWV time series (Figure 25). For comparison we estimated WWV with the XBT observations obtained on tracks west of 165°E. Both of our WWV time series estimates are admittedly crude; the ship data do not fully resolve temporal variability, and the XBT observations do not span the full ocean area between 165°E and the western boundary. Nevertheless, the result is instructive.

Net warm water transport across 165°E, estimated with the cruise data during the 1984–1986 reference period, was slightly eastward (7×10^6 m^3 s^{-1}; Figure 3), as was the case in July 1986. As was described in sections 3 and 4, however, direct WWV estimates suggest a modest 2.5-year accumulation of warm water during the ENSO buildup phase. This discrepancy might reflect periods of unresolved westward flow between cruises, and meridional convergence across 10°N and 10°S. For example, the Mindanao Current alone transports roughly 20×10^6 m^3 s^{-1} southward across 10°N [*Lukas et al.*, 1991].

In late 1986 the flow patterns were drastically altered when the western equatorial Pacific experienced significant westerly winds, reaching maximum strength around the 165°E meridian. One local result was the strong equatorial eastward jet observed in December (Figure 13) with a surface layer transport (2°N to 2°S) of 46×10^6 m^3 s^{-1}. Currents off the equator were also predominantly eastward in late 1986 and contributed an additional 42×10^6 m^3 s^{-1},

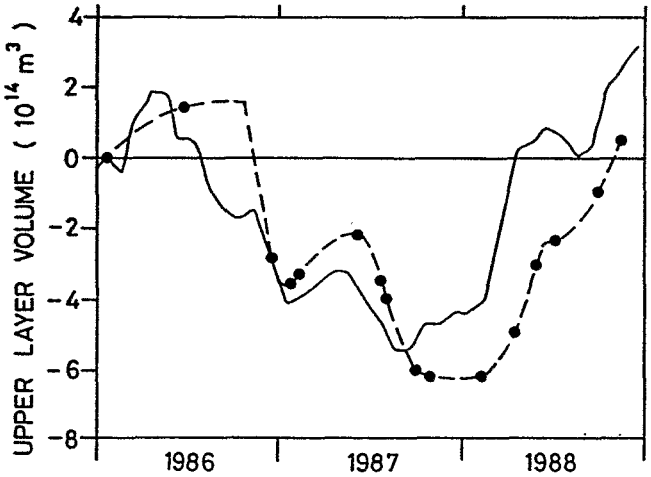

Fig. 25. Changes in warm water volume ($T > 25°C$) as estimated from XBT data (solid curve), and from the time integral of upper ocean ($\sigma_t > 23.5$) transport across 165°E (dashed curve, with dots showing the times of the cruises along 165°E from which the transport was estimated). See section 2 for details of the calculations.

for a net zonal transport (10°S to 10°N) of 88×10^6 m^3 s^{-1} (Figure 3). The tide gauge time series from the region (Figure 2) suggest that this pulse of eastward transport was relatively short lived: roughly from October 1986 to January 1987. (This is confirmed by the near-zero net transport estimate for SURTROPAC 7.) The transport-derived WWV decreases sharply during November–December because of the strong eastward flows (Figure 3). The XBT-derived WWV curve starts falling earlier in 1986, but we have no direct transport estimates for this time.

The strong eastward flows off the equator did not persist into 1987. Alternating zonal wind stress experienced from January to May 1987 led to reversals of the equatoral surface currents. Weak net transports across 165°E were observed for this period; the XBT-derived WWV grew slowly. Anomalous eastward flows were again observed about the equator on cruises in July and September 1987. Net eastward surface water transports in the 10°S to 10°N band were about 50×10^6 m^3 s^{-1} (Figure 3). It was argued in section 5 that these flows were the result both of local forcing by westerlies and of a first meridional mode Rossby wave propagating westward. These eastward surface currents continued to drain warm surface waters from the western Pacific (Figure 25). Both measures of WWV reached minimum values around October 1987.

Net zonal transport was weak from October 1987 to January 1988 when basin-wide indices were returning toward normal. XBT-derived WWV grew slowly through this period, while transport-derived WWV was nearly constant. A return of the trade winds during the La Niña period of March–May 1988 also forced anomalous currents, chiefly westward this time. Again, both local and remote forcing were invoked to account for the observed flow variations. WWV grew rapidly in response to significant westward net transport (Figure 3). Weakening trades in July 1988 coincided with reduced westward transport, slowing the recovery of the WWV, but sizable westward transports resumed during September–November 1988 with a return of strong trades, leading to the complete restoration of the pre–El Niño inventory of warm surface waters by the end of 1988.

Putting aside uncertainty due to our aliased observations, this analysis strongly suggests that, except for the very beginning of this ENSO event (July 1986), warm water volume variations of the western Pacific during 1986–1988 corresponded closely to surface layer zonal transport across 165°E. Interestingly, the present findings are quite consistent with the picture drawn from equatorial current meter mooring data by *McPhaden et al.* [1990], implying a correlation between flow at the equator and net zonal transport over the band 10°N to 10°S. Our present study finds that the transport variations were themselves caused by a combination of direct wind forcing and equatorial long waves propagating from the eastern Pacific. These findings, in addition, suggest explanations for observed zonal displacements of heat content [*Hénin and Donguy*, 1980] and SST [*McPhaden and Picaut*, 1990] maxima during ENSO cycles.

Of the many named low-latitude currents found at 165°E, only the subsurface countercurrents were observed on each cruise. All other currents vanished at one time or another during the 1986–1988 ENSO. The constancy of these flows, and indeed, their very existence remains a dynamical puzzle. (See *McPhaden* [1984] for a summary of observations and comparison with a linear model.)

As was previously observed near the equator between 143°E and 155°E, the upper layer (0–100 m) stratification at 165°E was frequently characterized by a thick isothermal layer containing a much shallower isohaline layer. *Lukas and Lindstrom* [1991] and *Godfrey and Lindstrom* [1989] argued that this so-called "barrier layer" structure is caused by surface circulation patterns and rainfall. Analysis of our 1984–1988 cruise data set at 165°E confirms the key roles of both, but highlights a complicated near-equatorial behavior which is sensitive to local winds and currents. Although we have confirmed the existence of the barrier layer in the warm pool as far east as 165°E, its precise role in the ENSO cycle was not established. Cruise sampling did not resolve the high-frequency response of the upper ocean to local winds, rainfall, and currents.

Acknowledgments. The present work represents the contributions from a great many scientists, technicians, shipboard personnal and support facilities. Foremost, we acknowledge the excellent work by the captains and crews of the R/V *Coriolis*, the *Xiangyanghong* #14 and #5, the *Oceanographer*, the *Korolev* and the *Natsushima*. Oceanographic cruise measurements were provided to us by S. Hayes (TEW 3), L. Talley (SAGA 2) and K. Muneyama (JENEX 1). Other data sets were supplied by K. Wyrtki and G. Mitchum (island sea level), J. O'Brien (FSU wind field), J. P. Rebert (XBT profiles), M. McPhaden (current meter data from 0°, 165°E) and the U.S. Climate Analysis Center. For permission to use all of these data sets we are very thankful. We had helpful discussions with many colleagues, including Y. du Penhoat, R. Millard, and F. Bahr. T.D., G.E. and M.-H.R. were supported by ORSTOM. J.T. and E.F.'s contributions were supported by the U.S. NOAA TOGA Program, grant NA85AA-D-AV117 to the Woods Hole Oceanographic Institution, and cooperative agreement NA-85-ABH-00032 with the University of Hawaii, respectively. Woods Hole Oceanographic Institution contribution 7747. University of Hawaii School of Ocean and Earth Science and Technology contribution 2809.

REFERENCES

Bahr, F., E. Firing, and J. Songnian, Acoustic Doppler current profiling in the western Pacific during the US-PRC TOGA cruises 2, 3, and 4, *JIMAR Data Rep. 5*, 199 pp., Joint Inst. for Mar. and Atmos. Res., Univ. of Hawaii, Honolulu, 1989.

Bahr, F., E. Firing, and J. Songnian, Acoustic Doppler current profiling in the western Pacific during the US-PRC TOGA cruises 5 and 6, *JIMAR Data Rep. 7*, 161 pp., Joint Inst. for Mar. and Atmos. Res., Univ. of Hawaii, Honolulu, 1990.

Barnes, C. A., D. F. Bumpus, and J. Lyman, Ocean circulation in Marshall Islands area, *Eos Trans. AGU, 29*, 871–876, 1948.

Bjerknes, J., Survey of El Niño 1957–58 in its relation to tropical Pacific meteorology, *Inter Am. Trop. Tuna Comm. Bull., 12*, 62 pp., 1966.

Blanchot, J., R. Le Borgne, A. Le Bouteiller, and M.-H. Radenac, Rapport de la campagne PROPPAC 1 du N.O. *Coriolis* (9 Sept.–8 Oct. 1987), Rapports de mission, Sciences de la mer, Océanographie, internal report, 10 pp., ORSTOM, Nouméa, New Caledonia, 1987. (Available from the authors.)

Cook, M., L. Mangum, R. Millard, G. Lamontagne, S. Pu, J. Toole, Z. Wang, K. Yang, and L. Zhao, Hydrographic observations from the US-PRC cooperative program in the western equatorial Pacific Ocean: Cruises 1–4, *Tech. Rep. WHOI-90-07*, 379 pp., Woods Hole Oceanogr. Inst., Woods Hole, Mass., Jan. 1990.

Delcroix, T., and C. Hénin, Observations of the Equatorial Intermediate Current in the western Pacific Ocean (165°E), *J. Phys. Oceanogr., 18*, 363–366, 1988.

Delcroix, T., and F. Masia, Atlas of sea surface temperature and salinity variations in the tropical Pacific (1969–1988), *Rapp. Sci. Tech., Ser. Sci. Mer Oceanogr. Phys. 2*, 151 pp., ORSTOM, Nouméa, New Caledonia, 1989.

Delcroix, T., G. Eldin, and C. Hénin, Upper ocean water masses and transports in the western tropical Pacific (165°E), *J. Phys. Oceanogr., 17*, 2248–2262, 1987.

Delcroix, T., J. Picaut, and G. Eldin, Equatorial Kelvin and Rossby waves evidenced in the Pacific Ocean through Geosat sea level and surface current anomalies, *J. Geophys. Res., 96*, suppl., 3249–3262, 1991.

Donguy, J. R., and C. Hénin, Two types of hydroclimatic conditions in the south-western Pacific, *Oceanol. Acta, 4*, 57–62, 1978.

Dorman, C. E., and R. H. Bourke, Precipitation over the Pacific Ocean, 30°S to 60°N, *Mon. Weather Rev., 107*, 896–910, 1979.

Eldin, G., On austral summer surface eastward flows at the equator in the western Pacific, in Proceedings of the U.S. TOGA Western Pacific Air-Sea Interaction Workshop, *U.S. TOGA 8*, edited by R. Lukas and P. Webster, pp. 177–182, University Corporation for Atmospheric Research, Boulder, Co., 1988.

Eldin, G., Coupes verticales des structures océaniques physiques à 165°E observées au cours des dix campagnes SURTROPAC, 1984–1988, *Rapp. Sci. Tech., Ser. Sci. Mer Oceanogr. Phys. 1*, 130 pp., ORSTOM, Nouméa, New Caledonia, 1989.

Eldin, G., and T. Delcroix, Vertical thermal structure variability along 165°E during the 1986–87 ENSO event, in *Proceedings of the Western Pacific International Meeting and Workshop on TOGA COARE*, edited by J. Picaut, R. Lukas, and T. Delcroix, pp. 269–281, ORSTOM, Nouméa, New Caledonia, 1989.

Elliot, W. P., and R. K. Reed, A climatological estimate of precipitation for the world ocean, *J. Clim. and Appl. Meteorol., 23*, 434–439, 1984.

Firing, E., Deep zonal currents in the central equatorial Pacific, *J. Mar. Res., 45*, 791–812, 1987.

Firing, E., R. Lukas, J. Sadler, and K. Wyrtki, Equatorial Undercurrent disappears during 1982–1983 El Niño, *Science, 222*, 1121–1123, 1983.

Gill, A., and E. Rasmusson, The 1982–1983 climate anomaly in the equatorial Pacific, *Nature, 305*, 229–234, 1983.

Godfrey, S., and E. Lindstrom, The heat budget of the equatorial western Pacific surface mixed layer, *J. Geophys. Res., 94*, 8007–8017, 1989.

Hayes, S. P., A comparison of geostrophic and measured velocities in the Equatorial Undercurrent, *J. Mar. Res., 40*, suppl., 219–229, 1982.

Hayes, S. P., L. J. Mangum, R. T. Barber, A. Huyer, and R. L. Smith, Hydrographic variability west of the Galapagos Islands during the 1982–83 El Niño, *Prog. Oceanogr., 17*, 137–162, 1986.

Hénin, C., Thermohaline structure variability along 165°E in the western tropical Pacific Ocean (January 1984 – January 1989), in *Proceedings of the Western Pacific International Meeting and Workshop on TOGA COARE*, edited by J. Picaut, R. Lukas, and T. Delcroix, pp. 155–164, ORSTOM, Nouméa, New Caledonia, 1989.

Hénin, C., and J. R. Donguy, Heat content changes within the mixed layer of the equatorial Pacific Ocean, *J. Mar. Res., 38*, 767–780, 1980.

Janoviak, J. E., and P. A. Arkin, Rainfall variations in the tropics during 1986–1989, as estimated from observations of cloud-top temperature, *J. Geophys. Res., 96*, suppl., 3359–3373, 1991.

Lander, M., A comparative analysis of the 1987 ENSO event, *Trop. Ocean-Atmos. Newsl. 49*, pp. 3–6, Nova Univ. Oceanogr. Center, Dania, Fl., 1987.

Leetmaa, A., D. W. Behringer, A. Huyer, R. L. Smith, and J. Toole, Hydrographic conditions in the eastern Pacific before, during and after the 1982/83 El Niño, *Prog. Oceanogr., 19*, 1–47, 1987.

Levitus, S., Climatological atlas of the world ocean, *NOAA Prof. Pap. 13*, 173 pp., U.S. Govt. Print. Office, Washington, D.C., 1982.

Lindstrom, E., R. Lukas, R. Fine, E. Firing, S. Godfrey, G. Meyers, and M. Tsuchiya, The western equatorial Pacific Ocean circulation study, *Nature, 330*, 533–537, 1987.

Lukas, R., and E. Lindstrom, The mixed layer of the western equatorial Pacific Ocean, *J. Geophys. Res., 96*, suppl., 3343–3357, 1991.

Lukas, R., E. Firing, P. Hacker, P. L. Richardson, C. A. Collins, R. Fine, and R. Gammon, Observations of the Mindanao Current during the Western Equatorial Pacific Ocean Circulation Study, *J. Geophys. Res., 96*, 7089–7104, 1991.

Magnier, Y., H. Rotschi, P. Rual, and C. Colin, Equatorial circu-

lation in the western Pacific, *Prog. Oceanogr., 6,* 29–46, 1973.
Mangum, L., J. Lynch, K. McTaggart, L. Stratton, and S. Hayes, CTD/O2 Data Measurements Collected on TEW (Transport of Equatorial Waters) Cruise, June – August 1987, *NOAA Data Rep. ERL PMEL-33,* 375 pp., U.S. Govt. Print. Office, Washington, D.C., June 1991.
McPhaden, M. J., On the dynamics of equatorial subsurface countercurrents, *J. Phys. Oceanogr., 14,* 1216–1225, 1984.
McPhaden, M. J., and S. P. Hayes, Variability in the eastern equatorial Pacific Ocean during 1986–1988, *J. Geophys. Res., 95,* 13,195–13,208, 1990.
McPhaden, M. J., and J. Picaut, El Niño–Southern Oscillation displacements of the western equatorial Pacific warm pool, *Science, 250,* 1385–1388, 1990.
McPhaden, M. J., S. P. Hayes, L. J. Mangum, and J. M. Toole, Variability in the western equatorial Pacific Ocean during the 1986–87 El Niño/Southern Oscillation event, *J. Phys. Oceanogr., 20,* 190–208, 1990.
Merle, J., H. Rotschi, and B. Voituriez, Zonal circulation in the tropical western Pacific at 170°E, Prof. Uda's Commemorative Papers, *Bull. Jpn. Soc. Fish. Oceanogr.,* Special Number, 91–98, 1969.
Meyers, G., and J. R. Donguy, An XBT network with merchant ships, *Trop. Ocean-Atmos. Newsl. 6,* pp. 6–7, Nova Univ. Oceanogr. Center, Dania, Fl., 1980.
Meyers, G., and J.R. Donguy, The North Equatorial Countercurrent and heat storage in the western Pacific Ocean during 1982–83, *Nature, 312,* 258–260, 1984.
Miller, L., R. E. Cheney, and B. C. Douglas, Geosat altimeter observations of Kelvin waves and the 1986–87 El Niño, *Science, 239,* 52, 1988.
Oudot, C., and B. Wauthy, Upwelling et dôme dans le Pacifique tropical occidental: Distributions physico-chimiques et biomasse végétale, *Cah. ORSTOM Ser. Oceanogr., 14-1,* 27–49, 1976.
Philander, S. G. H., Nonlinear coastal and equatorial jets, *J. Phys. Oceanogr., 9,* 739–747, 1979.
Philander, S. G. H., and R. C. Pacanowski, The generation of equatorial currents, *J. Geophys. Res., 85,* 1123–1136, 1980.
Picaut, J., and R. Tournier, Monitoring the 1979–1985 equatorial Pacific current transports with expendable bathythermograph data, *J. Geophys. Res., 96,* suppl., 3263–3277, 1991.
Rasmusson, E., and T. Carpenter, Variations in tropical sea surface temperature and surface wind fields associated with the Southern Oscillation/El Niño, *Mon. Weather Rev., 110,* 354–384, 1982.
Rotschi, H., P. Hisard, and F. Jarrige, Les eaux du Pacifique occidental à 170°E entre 20°S et 4°N, *Trav. Doc. ORSTOM, 19,* 113 pp., 1972.
Talley, L., and C. Collins, Physical, chemical, and CTD data, *Akademik Korolev,* 1 May 1987 – 9 June 1987, Ref. 88-10, 137 pp., Scripps Inst. of Oceanogr., La Jolla, Calif., 1988.
Toole, J. M., E. Zou, and R. C. Millard, On the circulation of the upper waters in the western equatorial Pacific Ocean, *Deep Sea Res., 35,* 1451–1482, 1988.
Tournier, R., Variabilité de la structure thermique et des courants à l'ouest et au centre de l'Océan Pacifique tropical de 1979 à 1985, *These,* 170 pp., Univ. Paris VI, 1989.
Tsuchiya, M., Upper waters of the intertropical Pacific Ocean, *Johns Hopkins Oceanogr. Stud., 4,* 50 pp., 1968.
Weisberg, R. H., and T. J. Weingartner, On the baroclinic response of the zonal pressure gradient in the equatorial Atlantic Ocean, *J. Geophys. Res., 91,* 11,717–11,725, 1986.
World Climate Research Program (WCRP), Scientific plan for the Tropical Ocean and Global Atmosphere program, *Publ. 3,* 146 pp., World Meteorol. Organ., Geneva, 1985.
Wyrtki, K., Sea level and seasonal fluctuations of the equatorial currents in the western Pacific Ocean, *J. Phys. Oceanogr., 4,* 91–103, 1974.
Wyrtki, K., El Niño—The dynamic response of the equatorial Pacific Ocean to atmospheric forcing, *J. Phys. Oceanogr., 5,* 572–584, 1975.
Wyrtki, K., The slope of sea level along the equator during the 1982/1983 El Niño, *J. Geophys. Res., 89,* 10,419–10,424, 1984.
Wyrtki, K., Water displacements in the Pacific and the genesis of El Niño cycles, *J. Geophys. Res., 90,* 7129–7132, 1985.
Wyrtki, K., and B. Kilonsky, Mean water and current structure during the Hawaii-to-Tahiti shuttle experiment, *J. Phys. Oceanogr., 14,* 242–254, 1984.
Wyrtki, K., and G. Meyers, The trade wind field over the Pacific Ocean, *J. Appl. Meteorol., 15,* 698–704, 1976.
Yoshida, K., A theory of the Cromwell Current and equatorial upwelling, *J. Oceanogr. Soc. Jpn., 15,* 154–170, 1959.

T. Delcroix and G. Eldin, Groupe SURTROPAC, ORSTOM, Nouméa, New Caledonia.
E. Firing, Department of Oceanography, University of Hawaii, 1000 Pope Road, Honolulu, HI 96822.
M.-H. Radenac, Groupe PROPPAC, ORSTOM, Nouméa, New Caledonia.
J. Toole, Woods Hole Oceanographic Institution, Woods Hole, MA 02543.

(Received May 10, 1991;
revised December 13, 1991;
accepted December 18, 1991.)